inherited thrombophilia: a study of 150 families. *Blood.* 1998; 92(7):2353-2358.
11. Eichinger S, Kyrle PA. Duration of anticoagulation after initial idiopathic venous thrombosis–the swinging pendulum: risk assessment to predict recurrence. *J Thromb Haemost.* 2009; 7(suppl 1):291-295.
12. Nomura T, Suehisa E, Kawasaki T, et al. Frequency of protein S deficiency in general Japanese population. *Thromb Res.* 2000; 100(5):367-371.
13. Dykes AC, Walker ID, McMahon AD, et al. A study of protein S antigen levels in 3788 healthy volunteers: influence of age, sex and hormone use, and estimate for prevalence of deficiency state. *Br J Haematol.* 2001;113(3):636-641.
14. Zama T, Murata M, Ono F, et al. Low prevalence of activated protein C resistance and coagulation factor V Arg506 to Gln mutation among Japanese patients with various forms of thrombosis, and normal individuals. *Int J Hematol.* 1996;65(1):71-78.
15. Isshiki I, Murata M, Watanabe R, et al. Frequencies of prothrombin 20210 G–>A mutation may be different among races—studies on Japanese populations with various forms of thrombotic disorders and healthy subjects. *Blood Coagul Fibrinolysis.* 1998;9(1):105-106.
16. Ozawa T, Niiya K, Sakuragawa N. Absence of factor V Leiden in the Japanese. *Thromb Res.* 1996;81(5):595-596.
17. Fujimura H, Kambayashi J, Monden M, et al. Coagulation factor V Leiden mutation may have a racial background. *Thromb Haemost.* 1995;74(5):1381-1382.
18. Miyata T, Kawasaki T, Fujimura H, et al. The prothrombin gene G20210A mutation is not found among Japanese patients with deep vein thrombosis and healthy individuals. *Blood Coagul Fibrinolysis.* 1998;9(5):451-452.
19. Suehisa E, Nomura T, Kawasaki T, et al. Frequency of natural coagulation inhibitor (antithrombin III, protein C and protein S) deficiencies in Japanese patients with spontaneous deep vein thrombosis. *Blood Coagul Fibrinolysis.* 2001;12(2):95-99.
20. Sakata T, Okamoto A, Mannami T, et al. Protein C and antithrombin deficiency are important risk factors for deep vein thrombosis in Japanese. *J Thromb Haemost.* 2004;2(3):528-530.
21. Kimura R, Honda S, Kawasaki T, et al. Protein S–K196E mutation as a genetic risk factor for deep vein thrombosis in Japanese patients. *Blood.* 2006;107(4):1737-1738.
22. Andersen BS, Steffensen FH, Sørensen HT, et al. The cumulative incidence of venous thromboembolism during pregnancy and puerperium. *Acta Obstet Gynecol Scand.* 1998;77(2):170-173.
23. Lindqvist P, Dahlbäck B, Marsál K. Thrombotic risk during pregnancy:a population study. *Obstet Gynecol.* 1999;94(4): 595-599.
24. Robertson L, Wu O, Langhorne P, et al. Thrombosis: Risk and Economic Assessment of Thrombophilia Screening (TREATS) Study. Thrombophilia in pregnancy: a systematic review. *Br J Haematol.* 2006;132:171-96.
25. Martinelli I, De Stefano V, Taioli E, et al. Inherited thrombophilia and first venous thromboembolism during pregnancy and puerperium. *Thromb Haemost.* 2002;87(5):791-795.
26. McColl M, Ramsay JE, Tait RC, et al. Risk factors for pregnancy associated venous thromboembolism. *Thromb Haemost.* 1997; 78(4):1183-1188.
27. Bates SM, Greer IA, Pabinger I, et al. American College of Chest Physicians. Venous thromboembolism, thrombophilia, antithrombotic therapy, and pregnancy: American College of Chest Physicians Evidence-Based Clinical Practice Guidelines (8th Edition). *Chest.* 2008;133(6 suppl):844S-886S.
28. Van Der Meer FJ, Rosendaal FR, Vandenbroucke JP, et al. Bleeding complications in oral anticoagulant therapy. An analysis of risk factors. *Arch Intern.* 1993;153(13):1557-1562.
29. Palareti G, Leali N, Coccheri S, et al. Bleeding complications of oral anticoagulant treatment: an inception-cohort, prospective collaborative study (ISCOAT). Italian Study on Complications of Oral Anticoagulant Therapy. *Lancet.* 1996;348(9025):423-428.
30. Douketis J, Tosetto A, Marcucci M, et al. Risk of recurrence after venous thromboembolism in men and women: patient level meta-analysis. *BMJ.* 2011;342:d813.
31. Baglin T, Luddington R, Brown K, et al. Incidence of recurrent venous thromboembolism in relation to clinical and thrombophilic risk factors: prospective cohort study. *Lancet.* 2003;362(9383): 523-526.
32. Christiansen SC, Cannegieter SC, Koster T, et al. Thrombophilia, clinical factors, and recurrent venous thrombotic events. *JAMA.* 2005;293(19):2352-2361.
33. Brouwers JL, Lijfering WM, Ten Kate MK, et al. High long-term absolute risk of recurrent venous thromboembolism in patients with hereditary deficiencies of protein S, protein C or antithrombin. *Thromb Haemost.* 2009;101(1):93-99.
34. Mitsuguro M, Sakata T, Okamoto A, et al. Usefulness of antithrombin deficiency phenotypes for risk assessment of venous thromboembolism: type I deficiency as a strong risk factor for venous thromboembolism. *Int J Hematol.* 2010;92(3):468-473.

J. Biochem. 2012;152(3):251–258 doi:10.1093/jb/mvs066

JB THE JOURNAL OF BIOCHEMISTRY

Binding of von Willebrand factor cleaving protease ADAMTS13 to Lys-plasmin(ogen)

Received February 2, 2012; accepted May 13, 2012; published online June 7, 2012

Yongchol Shin[1,2,*], Masashi Akiyama[1], Koichi Kokame[1], Kenji Soejima[3] and Toshiyuki Miyata[1,†]

[1]Department of Molecular Pathogenesis, National Cerebral and Cardiovascular Center, Suita, 5-7-1 Fujishirodai, Suita, Osaka 5658565, Japan; [2]Department of Applied Chemistry, Kogakuin University, 2665-1 Nakano-cho, Hachioji, Tokyo 1920015, Japan; and [3]Research Department 1, Chemo-Sero-Therapeutic Research Institute, 1314-1 Kawabe, Kyokushi, Kikuchi, Kumamoto 8691298, Japan

*Yongchol Shin, Department of Applied Chemistry, Kogakuin University, 2665-1 Nakano-cho, Hachioji, Tokyo 1920015, Japan. Tel: +81-42-673-1491, email: shin@cc.kogakuin.ac.jp

†Toshiyuki Miyata, Department of Molecular Pathogenesis, National Cerebral and Cardiovascular Center, 5-7-1 Fujishirodai, Suita, Osaka 5658565, Japan. Tel: +81-6-6833-5012 ext. 2512, Fax: +81-6-6835-1176, email: miyata@ri.ncvc.go.jp

The metalloprotease ADAMTS13 affects platelet adhesion and aggregation through depolymerization of von Willebrand factor (VWF) multimers. Identification of ADAMTS13-binding proteins would reveal the hitherto unrecognized mechanisms underlying microvascular thrombus. To identify ADAMTS13-binding proteins, we performed a yeast two-hybrid screen using the Cys-rich and spacer domains of ADAMTS13, the critical regions for the binding and cleavage of VWF, as a bait region. We identified Lys-plasminogen, an amino-terminal truncated form of plasminogen, as the binding protein to ADAMTS13. Intact Glu-plasminogen did not bind to ADAMTS13. Active-site blocked Lys-plasmin bound to ADAMTS13. Domain truncation of ADAMTS13 and elastase digest of plasminogen indicated that the Cys-rich and spacer domains of ADAMTS13 and the kringle 5 and protease domains of plasminogen served as the main binding sites. Biacore measurements revealed that Lys-plasminogen bound to ADAMTS13 with a K_d of $1.9 \pm 0.1 \times 10^{-7}$ M and Glu-plasminogen exhibited a significantly lower affinity to ADAMTS13. Specific activity measurements revealed that ADAMTS13 and Lys-plasmin were still active even after the binary complex was formed. The binding of ADAMTS13 to Lys-plasminogen may play an important role to localize these two proteases at sites of thrombus formation or vascular injury where the fibrinolytic system is activated.

Keywords: ADAMTS13/fibrinolysis/plasminogen/thrombotic thrombocytopenic purpura/von Willebrand factor.

Abbreviations: ADAMTS13, a disintegrin-like and metalloproteinase with thrombospondin type-1 motifs 13; APMSF, *p*-amidinophenyl methanesulfonyl fluoride; CUB, complement components C1r and C1s/urinary epidermal growth factor/bone morphogenic protein-1; Glu-Pg, Glu-plasminogen; HRP, horseradish peroxidase; Lys-Pg, Lys-plasminogen; mAb, monoclonal antibody; mini-Pg, mini-plasminogen; VWF, von Willebrand factor.

Platelet thrombus formation is dependent on the multimeric sizes of von Willebrand factor (VWF) under shear stress conditions. VWF multimers are depolymerized by plasma metalloprotease ADAMTS13. Thus, ADAMTS13 regulates the VWF-dependent platelet thrombus formation. Congenital or acquired deficiency of ADAMTS13 can cause thrombotic thrombocytopenic purpura that is characterized with thrombocytopoenia and microangiopathic haemolytic anaemia, sometimes accompanied with transient neurological dysfunction (*1–4*). ADAMTS13 has multiple discrete domains, comprising a metalloprotease domain (M), a disintegrin-like domain (D), a first thrombospondin type-1 repeat (T), a Cys-rich region (C), a spacer domain (S), seven consecutive T repeats and two CUB (Complement components C1r and C1s/urinary epidermal growth factor/bone morphogenic protein-1) domains (*5–7*).

ADAMTS13 cleaves a single specific peptide bond of Tyr^{1605}–Met^{1606} within the A2 domain of VWF under shear stress conditions *in vivo* or under denatured conditions *in vitro*. This restricted substrate specificity can be defined by several structural features in ADAMTS13. The C and S domains in ADAMTS13 play a critical role on the binding and cleavage of VWF, and the S domain seems to be highly important for the recognition of VWF (*8,9*). Studies using ADAMTS13 mutants and VWF peptides indicated cooperative and modular interaction of discrete segments of VWF with ADAMTS13 (*10–13*). The crystal structures of the DTCS domains showed three VWF-binding exosites on the linearly aligned discontinuous surfaces of the D, C and S domains (*14,15*). Two C-terminal CUB domains are also important for regulation of VWF cleavage *in vitro* as well as *in vivo* (*16–20*). Thus, the interaction between ADAMTS13 and VWF has been intensively investigated; however, the binding proteins for ADAMTS13 are not well known.

Fibrinolytic system in blood is involved in dissolution of blood clots and maintains a patent vascular system. The key component of the fibrinolytic system is plasmin that degrades fibrin clots. Plasmin is

generated from the inactive proenzyme, plasminogen, by cleavage of the Arg561–Val562 peptide bond. Two distinct physiological plasminogen activators, tissue type- or urokinase type-plasminogen activator, convert plasminogen to active plasmin on the fibrin or cell surface. Native plasminogen has N-terminal glutamic acid, designated Glu-plasminogen (Glu-Pg). Lys-plasminogen (Lys-Pg), an amino-terminal truncated form of plasminogen, is formed by the release of a 76-amino acid pre-activation peptide from intact Glu-Pg by the action of plasmin. Because Lys-Pg shows a more open conformation than Glu-Pg, plasminogen activators preferentially cleave Lys-Pg than Glu-Pg. To inhibit the fibrinolytic system, a plasminogen activator inhibitor-1 or α_2-plasmin inhibitor forms an inactive complex with plasminogen activator or plasmin, respectively (*21*).

In the present study, we performed a yeast two-hybrid screen using the critical regions, the C and S domains, for the VWF binding as a bait. The co-immunoprecipitation analysis, the far-western blotting and the Biacore measurement indicated that Lys-Pg is the binding protein to ADAMTS13. ADAMTS13 and Lys-plasmin were active even after the binary complex was formed. The binding of ADAMTS13 to Lys-Pg may play an important role to localize these two proteases at sites of thrombus formation or vascular injury where the fibrinolytic system is activated.

Materials and Methods

Yeast two-hybrid screen

The Matchmaker Two-hybrid System 3 (Clontech, Palo Alto, CA, USA) was used according to the manufacturer's instructions. A fragment encoding the C and S domains of human ADAMTS13 (amino acids 440–685) was used as the bait. cDNA libraries (Clontech) constructed from human liver and brain mRNA (1.3×10^8 and 1.4×10^7 clones, respectively) were screened. Insert DNA of positive clones was sequenced, and the sequence homologies were searched by basic local alignment search tool (BLAST).

Binding of ADAMTS13 to immobilized candidate proteins

The binding of ADAMTS13 (3 μg/ml) to immobilized proteins (9 μg/ml) was examined using microtiter plates. Bound ADAMTS13 to immobilized proteins was detected using anti-ADAMTS13 monoclonal antibody (mAb) WH2-22-1A, which recognizes the disintegrin-like domain (*22*), and horseradish peroxidase (HRP)-conjugated anti-mouse IgG antibody. Bound HRP activity was detected at 450 nm with a reference wavelength of 650 nm using 3,3′,5,5′-tetramethylbenzidine substrate (KPL, Gaithrburg, MD, USA) and a Multiskan Ascent microplate reader (Thermo, Waltham, MA, USA).

Co-immunoprecipitation analysis of ADAMTS13 with Glu-Pg or Lys-Pg

Human ADAMTS13 with a FLAG tag (ADAMTS13-FLAG) and two mutants, MD-FLAG constituting the M and D domains with the FLAG tag and MDTCS-FLAG constituting the M, D, T, C and S domains with the FLAG tag, were expressed in the culture medium using HeLa cells, as previously described (*8*). Culture medium containing each of those recombinant proteins was incubated with intact Glu-Pg (Calbiochem, Madison, WI, USA) and/or Lys-Pg (Calbiochem) in Tris-buffered saline (TBS: 50 mM Tris, 100 mM NaCl, pH 7.5) and immunoprecipitated with anti-FLAG M2 mAb-immobilized gel (Sigma-Aldrich, St. Louis, MO, USA). After washing with TBS containing 0.5% Tween-20 (TBS-T), proteins were eluted by the FLAG peptide, and subjected to SDS–PAGE for western blotting using anti-FLAG M2 mAb (Sigma) or anti-Pg mAb MAB2596 (R&D Systems, Minneapolis, MN, USA). Alternatively, we used the anti-Pg mAb and protein G-agarose (Sigma) for the co-immunoprecipitation analysis of purified ADAMTS13 (*22*) with Glu-Pg, Lys-Pg or *p*-amidinophenyl methanesulfonyl fluoride (APMSF)-treated Lys-plasmin (Calbiochem). Bound proteins were eluted with 100 mM glycine-HCl, pH 2.5, and then subjected to SDS–PAGE for western blotting using anti-ADAMTS13 mAb WH10, which recognizes the fourth thrombospondin type-1 repeat (*22*) or anti-Pg mAb MAB2596. Immunoblots were probed with HRP-conjugated anti-mouse IgG antibody. Protein bands were visualized using Western Lightning Chemiluminescence Reagent Plus (Perkin-Elmer, Waltham, MA, USA) on an image analyser LAS3000 (Fujifilm, Tokyo, Japan).

Identification of ADAMTS13 binding region in Lys-Pg

Lys-Pg (0.1 mg) was digested with porcine pancreatic elastase (5 μg; Sigma). The resulting mini-plasminogen (mini-Pg), a functionally active zymogen containing the kringle 5 and protease domains, and fragments containing the kringle 1–4 domains were obtained in the unbound and bound fractions, respectively, using a lysine-Sepharose column (GE Healthcare, Little Chalfont, UK) (*23*). Proteins were subjected to SDS–PAGE for N-terminal sequence analysis and transferred onto polyvinylidene difluoride membranes for far-western blotting. Proteins on the membranes were incubated with ADAMTS13. Bound ADAMTS13 was detected with the HRP-conjugated anti-ADAMTS13 polyclonal antibody (*22*) prepared using Peroxidase Labeling Kit-NH_2 (Dojindo, Kumamoto, Japan) and visualized using Western Lightning Chemiluminescence Reagent Plus on the image analyzer LAS3000.

Lys-Pg binding to ADAMTS13 using Biacore

The binding of Glu-Pg or Lys-Pg to ADAMTS13 was examined using a Biacore 2000 (GE healthcare, Piscataway, NJ, USA). ADAMTS13 was immobilized on a CM5 sensor chip with an amino coupling kit (GE healthcare) according to manufacturer's instructions. Approximately 500–600 resonance units (RU) of ADAMTS13 were covalently attached onto the chip. Lys-Pg (0.05, 0.1, 0.2, 0.4 and 0.8 μM) or Glu-Pg (0.4, 0.8, 1.6 and 3.2 μM) in 50 mM Tris, 100 mM NaCl, pH 7.5, containing 0.005% Tween-20 and 5 mM $CaCl_2$ was injected over the ADAMTS13-immobilized sensor chip at a flow rate of 20 μl/min for 2 min.

The sensor chip was regenerated with 50 mM Tris, 1 M NaCl, pH 7.5, containing 0.005% Tween-20 and 5 mM $CaCl_2$ for 1 min. The dissociation constants (K_d) at the equilibrium were obtained using several ligand concentrations with the BIA evaluation software. Each K_d value was obtained from four or three independent experiments using Lys-Pg or Glu-Pg, respectively.

Activity measurements of ADAMTS13 and plasmin in the complex

ADAMTS13 activity was measured using VWF (*24*) and synthetic fluorogenic substrate FRETS-VWF73 (Peptide Institute, Osaka, Japan) (*25*). For VWF assay, ADAMTS13 (15 ng/ml) was mixed with Glu-Pg (0.1 mg/ml), Lys-Pg (0.1 mg/ml) or bovine serum albumin (0.1 mg/ml) and incubated with guanidine-pretreated VWF multimers (2 mg/ml) for 30, 60 or 120 min at 37°C (*24*). The cleaved fragment with a molecular weight of 200 kDa was assessed by western blotting using HRP-conjugated anti-human VWF polyclonal antibody (DAKO, Carpinteria, CA, USA). For FRETS-VWF73 assay, ADAMTS13 (6.6×10^{-1} nM) was mixed with Glu-Pg (11, 110, 1100 nM) or Lys-Pg (12, 120, 1200 nM). After addition of FRETS-VWF73 (2 μM) to the mixture, increase in fluorescence was measured using Mx3000P System (Stratagene, La Jolla, CA, USA) with 340-nm excitation and 450-nm emission (*25*). The reaction rate was calculated by linear regression analysis of fluorescence over time from 0 min to 10 min using the PRISM software (GraphPad Software, San Diego, CA, USA). The relative activities were estimated from the activity of ADAMTS13 without Glu-Pg or Lys-Pg. To assess the plasmin activity, plasmin (20 nM) was preincubated with ADAMTS13 (40, 80, 200 nM) for 30 min at room temperature followed by the addition of S-2251 (1 mM). Plasmin activity was recorded as a change in absorbance at 405 nm with a reference wavelength of 492 nm during 30 min using the Multiskan Ascent microplate reader.

Results

Yeast two-hybrid screen for ADAMTS13

A yeast two-hybrid screen enabled us to identify more than 500 positive clones. A BLAST search for the insert DNA sequences identified approximately 200 genes, and 36 genes were categorized as membrane or secretory proteins. For further analysis, among these candidate genes, we selected nine secretory proteins that were commercially available or generously donated: Glu-Pg, biglycan (bovine), collagen type I, collagen type III, decorin (bovine), fibrinogen, laminin, histidine-rich glycoprotein and zinc-α2-glycoprotein. We found that ADAMTS13 was bound to immobilized Glu-Pg but not to the others (Fig. 1). The positive clone of human Pg contained a 676-bp cDNA fragment encoding the C-terminal 150 amino acids (amino acid residues 661–810) of the protease domain. ADAMTS13 also bound to Lys-Pg, an amino-terminal truncated form of Glu-Pg (Fig. 1).

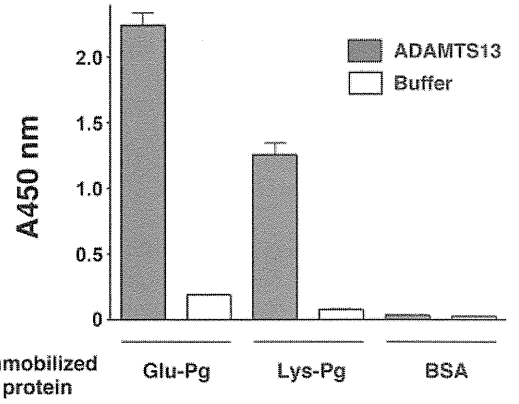

Fig. 1 Binding of ADAMTS13 to immobilized Glu-Pg and Lys-Pg. Microtitre wells were coated with Glu-Pg, Lys-Pg or BSA (each 9 μg/ml) and then incubated with or without ADAMTS13 (3 μg/ml). Bound ADAMTS13 was detected using anti-ADAMTS13 mAb WH2-22-1A (1 μg/ml) and HRP-conjugated anti-mouse IgG (0.25 μg/ml). After incubation with 3,3′,5,5′-tetramethylbenzidine substrate for 20 min, bound HRP activity was detected at 450 nm with a reference wavelength of 650 nm by a Multiskan Ascent microplate reader. The binding was expressed as the mean ± SD ($n = 3$). Grey bar, with ADAMTS13; white bar, without ADAMTS13.

ADAMTS13 binding to Pg

The binding of ADAMTS13 to Pg was examined by co-immunoprecipitation analysis. Anti-FLAG antibody immunoprecipitated ADAMTS13-FLAG with Lys-Pg but not with Glu-Pg (Fig. 2A). Next, anti-Pg antibody was used for the co-immunoprecipitation analysis. Again, ADAMTS13 was co-immunoprecipitated with only Lys-Pg but not with Glu-Pg (Fig. 2B). We found that APMSF-treated Lys-plasmin could be co-immunoprecipitated with ADAMTS13 (Fig. 2C). These results showed that Lys-Pg and Lys-plasmin but not Glu-Pg could bind to ADAMTS13. It is known that Glu-Pg and Lys-Pg have different conformational states in solution (*26*). We assumed that immobilized Glu-Pg had, in part, the conformational change on the plate surface. Microheterogeneity of Pg with or without carbohydrates attached to Asn289 is known (*27*). Doublets of Glu-Pg and Lys-Pg shown in Fig. 2 are likely explained by the carbohydrate difference.

Pg-binding domains in ADAMTS13

Because the C and S domains of ADAMTS13 were used as the bait, the Pg-binding regions would reside in the C and S domains. The co-immunoprecipitation analysis using MD-FLAG and MDTCS-FLAG of ADAMTS13 indicated that both could bind to Lys-Pg but not to Glu-Pg (Fig. 3A). The intensity of bound Lys-Pg was apparently lowest in MD-FLAG and highest in full-length ADAMTS13-FLAG, indicating the gradual loss of affinity in domain truncation. The dose-dependent binding experiments showed that Lys-Pg bound to MDTCS-FLAG at a lower concentration (4 nM) than MD-FLAG (Fig. 3B). Although the Lys-Pg binding to MDTCS-FLAG was saturated at 40 nM, the binding to MD-FLAG was not saturated at the same concentration. The results of the yeast two-hybrid screen and the co-immunoprecipitation

analysis together revealed that the C and S domains in ADAMTS13 are necessary for strong binding to Lys-Pg. Because the M domain of ADMATS13 has two glycosylation sites (*28*), doublets of MD-FLAG might be caused by the difference of carbohydrate. Alternatively, we cannot exclude the possibility of limited proteolysis of MD-FLAG.

ADAMTS13-binding region in Lys-Pg

Elastase has been used for the domain isolation of Pg (*23*), and the resulting fragments containing kringle 1 and 4 domains can bind to lysine-Sepharose. We digested Pg with elastase and unbound and bound fractions for lysine-Sepharose were obtained. Lys-Pg, elastase-digested Lys-Pg and lysine-Sepharose unbound and bound fractions of elastase-digested Lys-Pg were subjected to SDS–PAGE (Fig. 4A) for the far-western blotting using ADAMTS13 as the ligand (Fig. 4B). As a result, ADAMTS13 bound to three bands: Lys-Pg, a 40-kDa fragment and a 32-kDa fragment (Fig. 4B, right). N-terminal sequence analysis revealed that the lysine-Sepharose bound 40-kDa fragment was the kringle 4 and 5 and protease domains (K4-K5-P) and the lysine-Sepharose unbound 32-kDa fragment was mini-Pg, which consists of the kringle 5 and protease domains (K5-P). Thus, we concluded that ADAMTS13 bound to mini-Pg but not to the kringle 1–4 domains. This was compatible with the result of the yeast two-hybrid screen that the positive clone contained C-terminal 150 residues of the protease domain of Pg.

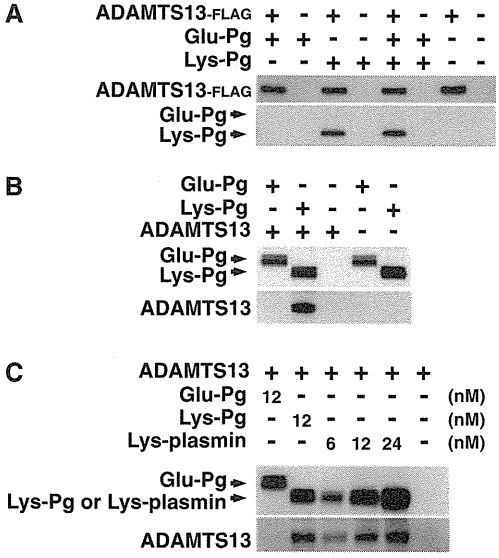

Fig. 2 Binding of ADAMTS13 to Lys-Pg. (**A**) Co-immunoprecipitation using anti-FLAG mAb. The culture medium containing ADAMTS13-FLAG was incubated with Glu-Pg (100 nM) and/or Lys-Pg (100 nM), and then anti-FLAG mAb-immobilized gel was added to recover bound complexes. Proteins in the complexes were subjected to SDS–PAGE for western blotting using anti-FLAG mAb or anti-Pg mAb. The result is representative of three experiments. (**B** and **C**) Co-immunoprecipitation using anti-Pg mAb. (B) Purified ADAMTS13 (6.7 nM) was incubated with Glu-Pg (12 nM) or Lys-Pg (12 nM), and then anti-Pg mAb was added. Immunocomplexes were subjected to SDS–PAGE for western blotting using anti-Pg mAb or anti-ADAMTS13 mAb WH10. (C) Binding of ADAMTS13 to active-site inhibited plasmin. ADAMTS13 (6.7 nM) was first incubated with Glu-Pg (12 nM), Lys-Pg (12 nM) and APMSF-treated plasmin (6, 12 and 24 nM) and then incubated with anti-Pg mAb. The immunocomplexes were analysed as described in (B). The result is representative of three experiments.

Binding of Pg to immobilized ADAMTS13 using Biacore

ADAMTS13 was immobilized on the sensor chip, and the binding of Glu-Pg or Lys-Pg to ADAMTS13 was measured by recording the changes in surface plasmon resonance upon injection of Pgs using Biacore. We observed that Lys-Pg bound to immobilized ADAMTS13 in the dose-dependent manner (Fig. 5A), whereas Glu-Pg could not significantly bind to ADAMTS13 (Fig. 5B). Lys-Pg exhibited a higher binding affinity to ADAMTS13 with a K_d of $1.9 \pm 0.1 \times 10^{-7}$ M (the mean ± SD) than Glu-Pg with a K_d of $5.5 \pm 2.7 \times 10^{-6}$ M (the mean ± SD).

Plasmin and ADAMTS13 activities in the complex

The C and S domains of ADAMTS13 were necessary for the recognition and cleavage of VWF. Therefore, the Lys-Pg binding to ADAMTS13 may affect the ADAMTS13 activity. We examined the effects of Lys-Pg on the ADAMTS13 activity. We found that Lys-Pg did not affect the ADAMTS13 activity towards the natural substrate VWF (Fig. 6A) and the synthetic

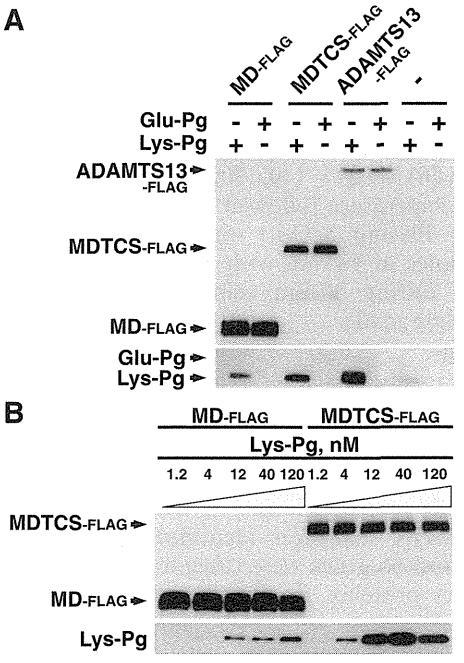

Fig. 3 Binding of ADAMTS13 and its truncated mutants to Glu-Pg or Lys-Pg. (**A**) Binding of MD-FLAG, MDTCS-FLAG and ADAMTS13-FLAG to Glu-Pg and Lys-Pg. The culture medium containing MD-FLAG, MDTCS-FLAG or ADAMTS13-FLAG was incubated with Glu-Pg (35 nM) or Lys-Pg (35 nM). The complex was immunoprecipitated and then probed with anti-FLAG mAb or anti-Pg mAb. The result is representative of three experiments. (**B**) Dose-dependent binding of Lys-Pg to MD-FLAG and MDTCS-FLAG. Lys-Pg (1.2, 4, 12, 40, 120 nM) was incubated with the culture medium containing MD-FLAG or MDTCS-FLAG. The complex was analysed as described in (A). The result is representative of three experiments.

substrate FRETS-VWF73 (Fig. 6B). The plasmin activity was also not affected by ADAMTS13 even in the 10-fold molar excess of plasmin concentration (Fig. 6C).

Discussion

In this study, we have demonstrated that ADAMTS13 binds to Lys-Pg, the N-terminal truncated form of Pg. This interaction was firstly identified by yeast two-hybrid screen of human liver and brain cDNA libraries using the C and S domains of ADAMTS13 as the bait. This interaction was further demonstrated by the co-immunoprecipitation analysis, the far-western blotting and the Biacore system.

Under physiological conditions, Lys-Pg and Lys-plasmin are not present in circulating blood (*29*). However, in patients undergoing thrombolytic therapy using tissue plasminogen activator, low, but significant, amount of Lys-Pg was detected (*29*). Tissue plasminogen activator can be released from endothelium storage upon venous occlusion, stimulation of epinephrine or desmopressin acetate, and physical exercise. Therefore, under these conditions, Lys-Pg may be locally generated by tissue plasminogen activator and the complex of ADAMTS13 with Lys-Pg might be locally formed, thereby regulating the thrombus formation through VWF cleavage and fibrin degradation.

Physical properties of Glu-Pg and Lys-Pg are quite different. Analysis using small-angle scattering revealed that Glu-Pg has a form with the overall shape of a prolate ellipsoid by interaction between the domains in Pg (*26*). ADAMTS13 can exclusively bind to Lys-Pg but not to Glu-Pg, indicating that ADAMTS13 distinguishes the specific conformation of Lys-Pg. It is known that the conformation of plasmin is resembled to that of Lys-Pg but not Glu-Pg. It is consistent with our result that not only Lys-Pg but also Lys-plasmin can bind to ADAMTS13. Quite recently, the crystal structure of human Glu-Pg has been determined (*30*). The structure clearly showed that seven domains consisting of a Pan-apple domain, five kringle domains and a serine protease domain are loosely clustered in a diamond-shaped zig-zag assembly. Notably, the serine protease domain has a contact with kringle 2 and 4 domains. Although the structure of Lys-Pg remains to be determined, these domain contacts may differ between Glu-Pg and Lys-Pg, resulting in preferable binding of ADAMTS13 to Lys-Pg.

Recently, it was shown that ADAMTS13 is a substrate of plasmin *in vitro* (*31*, *32*). We performed a preliminary experiment as to the ADAMTS13 cleavage with plasmin (data not shown). We found that plasmin cleaved ADAMTS13 into several fragments, and the profile of those fragments was very similar to those previously reported by Crawley *et al.* (*31*) and Hiura *et al.* (*32*). Previous studies showed that the ADAMTS13 activity was progressively decreased by plasmin digestion (*31*, *32*). As for the cleavage sites, plasmin cleaved three peptide bonds, R257-A258 in the metalloprotease domain, R888-T889 in the T4 domain and R1176-R1177 in the T8 domain, but it did not cleave any peptide bonds in the C and S domains

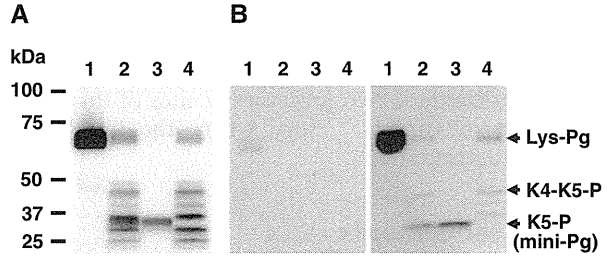

Fig. 4 Binding of ADAMTS13 to mini-Pg. Lys-Pg (lane 1, 1.28 μg protein), elastase-digested Lys-Pg (lane 2, 1.28 μg protein), and lysine-Sepharose unbound (mini-Pg, lane 3, 0.64 μg protein) and bound (several fragments containing kringle 1–4 domains, lane 4, 1.28 μg protein) fractions of elastase-digested Lys-Pg were subjected to SDS-PAGE and transferred onto polyvinylidene difluoride membranes. (A) Coomassie Brilliant Blue staining for N-terminal sequence analysis. The N-terminal sequences of 32-kDa (lane 3) and 40-kDa (lane 4) bands were $V^{461}APPP^{465}$ and $V^{374}QDXY^{378}$, respectively, indicating that those were mini-Pg (K5-P) and a fragment consisting of the kringle 4 and 5 and protease domains (K4-K5-P), respectively. (**B**) Far-western blotting. The membrane was incubated without (left) or with (right) ADAMTS13 (4.5 μg/ml). Bound ADAMTS13 was detected by the HRP-conjugated anti-ADAMTS13 polyclonal antibody. The result is representative of three experiments.

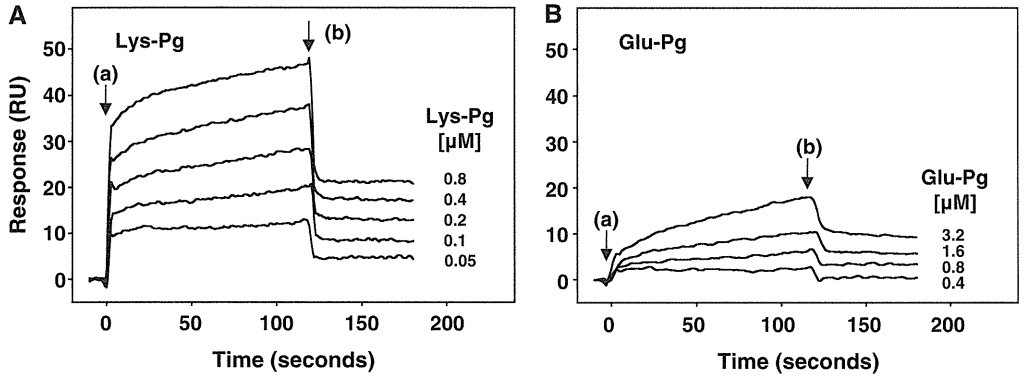

Fig. 5 Binding of Lys-Pg and Glu-Pg to immobilized ADAMTS13 using Biacore. ADAMTS13 was immobilized onto the sensor chip, and Lys-Pg (**A**: 0.05, 0.1, 0.2, 0.4 and 0.8 μM) or Glu-Pg (**B**: 0.4, 0.8, 1.6 and 3.2 μM) was injected over the ADAMTS13-immobilized sensor chip at a flow rate of 20 μl/min for 2 min. The *arrows* indicate the beginning (a) and the end (b) of the application of Pgs. Sensorgrams are shown from a typical experiment, which was repeated at least three times with similar results.

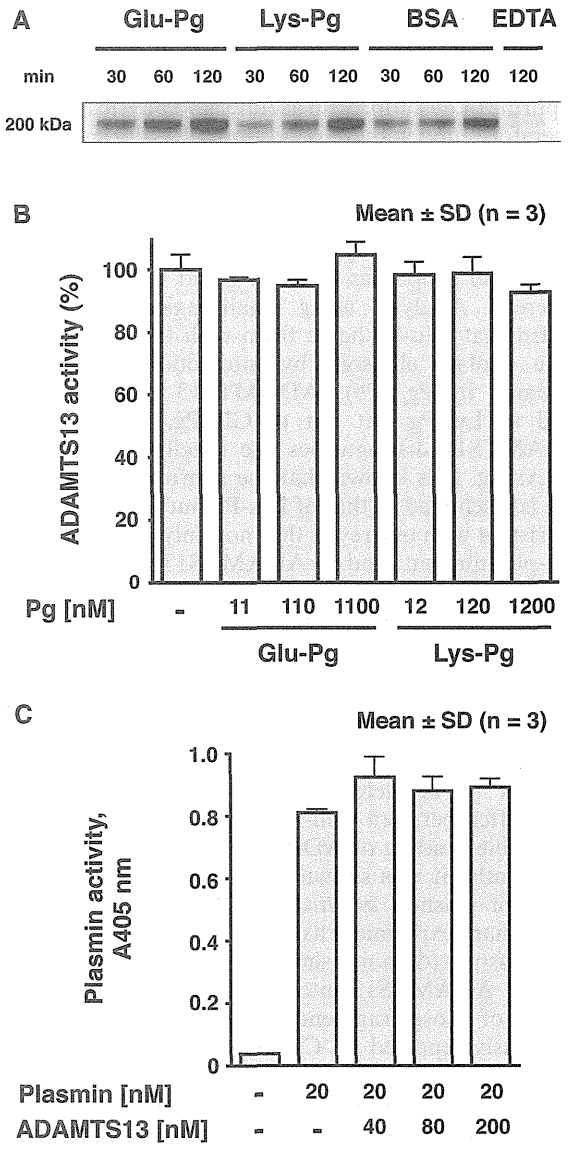

Fig. 6 Plasmin and ADAMTS13 activities in the complex. ADAMTS13 activity was assessed by the appearance of a 200-kDa fragment of VWF using western blotting (**A**) and by FRETS-VWF73 (**B**) as described under the 'Materials and Methods' section. Briefly, for VWF assay, ADAMTS13 was mixed with Glu-Pg, Lys-Pg or BSA and incubated with guanidine-pretreated VWF multimers at 37°C. The cleaved fragment was assessed by western blotting using HRP-conjugated anti-human VWF polyclonal antibody. For FRETS-VWF73 assay, ADAMTS13 was mixed with Glu-Pg or Lys-Pg and was incubated with FRETS-VWF73. Increase in fluorescence was measured with 340-nm excitation and 450-nm emission. The reaction rate was calculated by linear regression analysis of fluorescence over time from 0 min to 10 min. The relative activities were estimated from the activity of ADAMTS13 without Glu-Pg or Lys-Pg. The plasmin activity was assessed using S-2251 as substrate (C) as described under the 'Materials and Methods' section. Briefly, plasmin was preincubated with ADAMTS13 followed by the addition of S-2251. Plasmin activity was recorded as a change in absorbance at 405 nm during 30 min.

(*32*). Therefore, the fragments generated from plasmin-digested ADAMTS13 are likely to have intact C and S domains that are necessary for the plasminogen binding.

Fibrin and endothelial proteins, annexin II and α-enolase, bind to Lys-Pg through its lysine-binding site in the kringle domains (*33*, *34*). Since Lys-Pg can bind to cultured endothelial cells in a rapid and reversible fashion via the lysine-binding sites, annexin II and α-enolase are thought to be endothelial receptors for Pg. Interestingly, ADAMTS13 binds to the elastase fragment consisting of the kringle 5 and the serine protease domain of Lys-Pg. Taken together with the result of yeast two-hybrid screen, our observations suggest that the Lys-Pg binding to ADAMTS13 is a novel binding mechanism through the serine protease domain of Lys-Pg. Since the binding site of Lys-Pg to ADAMTS13 is different from that of Lys-Pg to fibrin or endothelial cells, the ADAMTS13–Lys-Pg complex might be anchored to the cells through the kringle domains of the complex. Additionally, we have demonstrated that ADAMTS13 is still active after the complex is formed. Recently, it has been shown that binding of ADAMTS13 to endothelial cells enhances its enzymatic activity (*35*).

In this study, we demonstrated ADAMTS13 binding to Lys-Pg. The physiological role of this binary complex is not clear at present; however, it might contribute to localize these two proteases at sites of thrombus formation or vascular injury where the fibrinolytic system is activated.

Acknowledgements

We thank Miyuki Kuroi for her excellent technical assistance. We thank Dr. T. Koide at University of Hyogo for human histidine-rich glycoprotein and Dr. I. Ohkubo at Shiga University of Medical Science for human zinc-α2-glycoprotein.Y.S. designed and performed research, analysed and interpreted data, and wrote the paper; K.K. interpreted data; M.A. and K.S. contributed the substantial experimental materials; T.M. designed research, interpreted data and wrote the paper.

Funding

This work was supported in part by a Grant-in-Aid for scientific research from the Ministry of Health, Labor and Welfare of Japan (to T.M.); the Ministry of Education, Culture, Sports, Science and Technology of Japan (to K.K., M.A. and T.M.); and the Program for Promotion of Fundamental Studies in Health Sciences of the National Institute of Biomedical Innovation (NIBIO) of Japan (to T.M.). Shin was a research resident supported by the Japan Health Sciences Foundation at the National Cerebral and Cardiovascular Center Research Institute.

Conflict of interest

K.S. is an employee of Chemo-Sero-Therapeutic Research Institute. The National Cerebral and Cardiovascular Center where T.M. and K.K. (inventors) belong has an awarded patent on the use of reagent, FRETS-VWF73. The other authors state that they have no conflict of interest.

References

1. Moake, J.L. (1998) Moschcowitz, multimers, and metalloprotease. *N. Engl. J. Med.* **339**, 1629–1631
2. Tsai, H.M. (2006) Current concepts in thrombotic thrombocytopenic purpura. *Annu. Rev. Med.* **57**, 419–436
3. Miyata, T., Kokame, K., Banno, F., Shin, Y., and Akiyama, M. (2007) ADAMTS13 assays and

ADAMTS13-deficient mice. *Curr. Opin. Hematol.* **14**, 277–283

4. Hughes, C., McEwan, J.R., Longair, I., Hughes, S., Cohen, H., Machin, S., and Scully, M. (2009) Cardiac involvement in acute thrombotic thrombocytopenic purpura: association with troponin T and IgG antibodies to ADAMTS 13. *J. Thromb. Haemost.* **7**, 529–536
5. Soejima, K., Mimura, N., Hirashima, M., Maeda, H., Hamamoto, T., Nakagaki, T., and Nozaki, C. (2001) A novel human metalloprotease synthesized in the liver and secreted into the blood: possibly, the von Willebrand factor-cleaving protease? *J. Biochem.* **130**, 475–480
6. Zheng, X., Chung, D., Takayama, T.K., Majerus, E.M., Sadler, J.E., and Fujikawa, K. (2001) Structure of von Willebrand factor-cleaving protease (ADAMTS13), a metalloprotease involved in thrombotic thrombocytopenic purpura. *J. Biol. Chem.* **276**, 41059–41063
7. Levy, G.G., Nichols, W.C., Lian, E.C., Foroud, T., McClintick, J.N., McGee, B.M., Yang, A.Y., Siemieniak, D.R., Stark, K.R., Gruppo, R., Sarode, R., Shurin, S.B., Chandrasekaran, V., Stabler, S.P., Sabio, H., Bouhassira, E.E., Upshaw, J.D. Jr, Ginsburg, D., and Tsai, H.M. (2001) Mutations in a member of the ADAMTS gene family cause thrombotic thrombocytopenic purpura. *Nature* **413**, 488–494
8. Soejima, K., Matsumoto, M., Kokame, K., Yagi, H., Ishizashi, H., Maeda, H., Nozaki, C., Miyata, T., Fujimura, Y., and Nakagaki, T. (2003) ADAMTS-13 cysteine-rich/spacer domains are functionally essential for von Willebrand factor cleavage. *Blood* **102**, 3232–3237
9. Zheng, X., Nishio, K., Majerus, E.M., and Sadler, J.E. (2003) Cleavage of von Willebrand factor requires the spacer domain of the metalloprotease ADAMTS13. *J. Biol. Chem.* **278**, 30136–30141
10. Gao, W., Anderson, P.J., and Sadler, J.E. (2008) Extensive contacts between ADAMTS13 exosites and von Willebrand factor domain A2 contribute to substrate specificity. *Blood* **112**, 1713–1719
11. de Groot, R., Bardhan, A., Ramroop, N., Lane, D.A., and Crawley, J.T. (2009) Essential role of the disintegrin-like domain in ADAMTS13 function. *Blood* **113**, 5609–5616
12. Zanardelli, S., Chion, A.C., Groot, E., Lenting, P.J., McKinnon, T.A., Laffan, M.A., Tseng, M., and Lane, D.A. (2009) A novel binding site for ADAMTS13 constitutively exposed on the surface of globular VWF. *Blood* **114**, 2819–2828
13. Feys, H.B., Anderson, P.J., Vanhoorelbeke, K., Majerus, E.M., and Sadler, J.E. (2009) Multi-step binding of ADAMTS-13 to von Willebrand factor. *J. Thromb. Haemost.* **7**, 2088–2095
14. Akiyama, M., Takeda, S., Kokame, K., Takagi, J., and Miyata, T. (2009) Production, crystallization and preliminary crystallographic analysis of an exosite-containing fragment of human von Willebrand factor-cleaving proteinase ADAMTS13. *Acta. Crystallogr. Sect. F Struct. Biol. Cryst. Commun.* **65**, 739–742
15. Akiyama, M., Takeda, S., Kokame, K., Takagi, J., and Miyata, T. (2009) Crystal structures of the noncatalytic domains of ADAMTS13 reveal multiple discontinuous exosites for von Willebrand factor. *Proc. Natl. Acad. Sci. USA* **106**, 19274–19279
16. Banno, F., Kaminaka, K., Soejima, K., Kokame, K., and Miyata, T. (2004) Identification of strain-specific variants of mouse Adamts13 gene encoding von Willebrand factor-cleaving protease. *J. Biol. Chem.* **279**, 30896–30903
17. Majerus, E.M., Anderson, P.J., and Sadler, J.E. (2005) Binding of ADAMTS13 to von Willebrand factor. *J. Biol. Chem.* **280**, 21773–21778
18. Tao, Z., Peng, Y., Nolasco, L., Cal, S., Lopez-Otin, C., Li, R., Moake, J.L., Lopez, J.A., and Dong, J.F. (2005) Recombinant CUB-1 domain polypeptide inhibits the cleavage of ULVWF strings by ADAMTS13 under flow conditions. *Blood* **106**, 4139–4145
19. Zhang, P., Pan, W., Rux, A.H., Sachais, B.S., and Zheng, X.L. (2007) The cooperative activity between the carboxyl-terminal TSP1 repeats and the CUB domains of ADAMTS13 is crucial for recognition of von Willebrand factor under flow. *Blood* **110**, 1887–1894
20. Banno, F., Chauhan, A.K., Kokame, K., Yang, J., Miyata, S., Wagner, D.D., and Miyata, T. (2009) The distal carboxyl-terminal domains of ADAMTS13 are required for regulation of in vivo thrombus formation. *Blood* **113**, 5323–5329
21. Rijken, D.C. and Lijnen, H.R. (2009) New insights into the molecular mechanisms of the fibrinolytic system. *J. Thromb. Haemost.* **7**, 4–13
22. Soejima, K., Nakamura, H., Hirashima, M., Morikawa, W., Nozaki, C., and Nakagaki, T. (2006) Analysis on the molecular species and concentration of circulating ADAMTS13 in blood. *J. Biochem.* **139**, 147–154
23. Sottrup-Jensen, L., Claeys, H., Zajdel, M., Petersen, T.E., and Magnusson, S. (1978) The primary structure of human plasminogen: isolation of two lysine-binding fragments and one "mini"-plasminogen (MW 38,000) by elastase-catalyzed-specific limited proteolysis *Progress in Chemical Fibrinolysis and Thrombolysis* (Davidson, J.F., Rowan, R.M., Samama, M.M., and Desnoyers, P.C., eds.), pp. 191–209, Raven Press, New York
24. Tsai, H.M. (1996) Physiologic cleavage of von Willebrand factor by a plasma protease is dependent on its conformation and requires calcium ion. *Blood* **87**, 4235–4244
25. Kokame, K., Nobe, Y., Kokubo, Y., Okayama, A., and Miyata, T. (2005) FRETS-VWF73, a first fluorogenic substrate for ADAMTS13 assay. *Br. J. Haematol.* **129**, 93–100
26. Mangel, W.F., Lin, B.H., and Ramakrishnan, V. (1990) Characterization of an extremely large, ligand-induced conformational change in plasminogen. *Science* **248**, 69–73
27. Castellino, F.J. and Powell, J.R. (1981) Human plasminogen. *Methods Enzymol.* **80**, Pt C, 365–378
28. Zhou, W. and Tsai, H.M. (2009) N-Glycans of ADAMTS13 modulate its secretion and von Willebrand factor cleaving activity. *Blood* **113**, 929–935
29. Holvoet, P., Lijnen, H.R., and Collen, D. (1985) A monoclonal antibody specific for Lys-plasminogen. Application to the study of the activation pathways of plasminogen in vivo. *J. Biol. Chem.* **260**, 12106–12111
30. Low, R.H., Caradoc-Davies, T., Cowieson, N., Horvath, A.J., Quek, A.J., Encarnacao, J.A., Steer, D., Cowan, A., Zhang, Q., Lu, B.G., Pike, R.N., Smith, A.I., Coughlin, P.B., and Whisstock, J.C. (2012) The X-ray crystal structure of full-length human plasminogen. *Cell Rep.* **1**, 185–190
31. Crawley, J.T., Lam, J.K., Rance, J.B., Mollica, L.R., O'Donnell, J.S., and Lane, D.A. (2005) Proteolytic inactivation of ADAMTS13 by thrombin and plasmin. *Blood* **105**, 1085–1093

32. Hiura, H., Matsui, T., Matsumoto, M., Hori, Y., Isonishi, A., Kato, S., Iwamoto, T., Mori, T., and Fujimura, Y. (2010) Proteolytic fragmentation and sugar chains of plasma ADAMTS13 purified by a conformation-dependent monoclonal antibody. *J. Biochem.* **148**, 403–411
33. Miles, L.A., Dahlberg, C.M., Plescia, J., Felez, J., Kato, K., and Plow, E.F. (1991) Role of cell-surface lysines in plasminogen binding to cells: identification of alpha-enolase as a candidate plasminogen receptor. *Biochemistry* **30**, 1682–1691
34. Hajjar, K.A., Jacovina, A.T., and Chacko, J. (1994) An endothelial cell receptor for plasminogen/tissue plasminogen activator. *I. Identity with annexin II. J. Biol. Chem.* **269**, 21191–21197
35. Vomund, A.N. and Majerus, E.M. (2009) ADAMTS13 bound to endothelial cells exhibits enhanced cleavage of von Willebrand factor. *J. Biol. Chem.* **284**, 30925–30932

Neurol Sci (2012) 33:1107–1115
DOI 10.1007/s10072-011-0913-9

ORIGINAL ARTICLE

ADAMTS13 gene deletion enhances plasma high-mobility group box1 elevation and neuroinflammation in brain ischemia–reperfusion injury

Masayuki Fujioka · Takafumi Nakano · Kazuhide Hayakawa · Keiichi Irie · Yoshiharu Akitake · Yuya Sakamoto · Kenichi Mishima · Carl Muroi · Yasuhiro Yonekawa · Fumiaki Banno · Koichi Kokame · Toshiyuki Miyata · Kenji Nishio · Kazuo Okuchi · Katsunori Iwasaki · Michihiro Fujiwara · Bo K. Siesjö

Received: 13 August 2011 / Accepted: 20 December 2011 / Published online: 3 January 2012

Abstract Highly adhesive glycoprotein von Willebrand factor (VWF) multimer induces platelet aggregation and leukocyte tethering or extravasation on the injured vascular wall, contributing to microvascular plugging and inflammation in brain ischemia–reperfusion. A disintegrin and metalloproteinase with thrombospondin type-1 motifs 13 (ADAMTS13) cleaves the VWF multimer strand and reduces its prothrombotic and proinflammatory functions. Although ADAMTS13 deficiency is known to amplify post-ischemic cerebral hypoperfusion, there is no report available on the effect of ADAMTS13 on inflammation after brain ischemia. We investigated if ADAMTS13 deficiency intensifies the increase of extracellular HMGB1, a hallmark of post-stroke inflammation, and exacerbates brain injury after ischemia–reperfusion. ADAMTS13 gene knockout (KO) and wild-type (WT) mice were subjected to 30-min middle cerebral artery occlusion (MCAO) and 23.5-h reperfusion under continuous monitoring of regional cerebral blood flow (rCBF). The infarct volume, plasma high-mobility group box1 (HMGB1) level, and immunoreactivity of the ischemic cerebral cortical tissue (double immunofluorescent labeling) against HMGB1/NeuN (neuron-specific nuclear protein) or HMGB1/MPO (myeloperoxidase) were estimated 24 h after MCAO. ADAMTS 13KO mice had larger brain infarcts compared with WT 24 h after MCAO ($p < 0.05$). The rCBF during reperfusion decreased more in ADAMTS13KO mice. The plasma HMGB1 increased more in ADAMTS13KO mice than in WT after ischemia–reperfusion ($p < 0.05$). Brain ischemia induced more prominent activation of inflammatory cells co-expressing HMGB1 and MPO and more marked neuronal death in the cortical ischemic penumbra of ADAMTS13KO mice. ADAMTS13 deficiency may enhance systemic and brain inflammation associated with HMGB1 neurotoxicity, and aggravate brain damage in mice after brief focal ischemia. We hypothesize that ADAMTS13 protects brain from ischemia–reperfusion injury by regulating VWF-dependent inflammation as well as microvascular plugging.

Keywords Brain ischemia–reperfusion · High-mobility group box1 · ADAMTS13 · Inflammation · Von Willebrand factor · Thrombotic thrombocytopenic purpura

M. Fujioka (✉) · T. Nakano · K. Hayakawa · K. Irie · Y. Akitake · Y. Sakamoto · K. Mishima · C. Muroi · K. Iwasaki · M. Fujiwara
Department of Neuropharmacology, Faculty of Pharmaceutical Sciences, Fukuoka University, Fukuoka, Japan
e-mail: mfujioka_2000_99@yahoo.co.jp

M. Fujioka
Stroke Center, Helios General Hospital Aue, Dresden University of Technology, Dresden, Saxony, Germany

M. Fujioka · C. Muroi · Y. Yonekawa
Department of Neurosurgery, University of Zurich, Zurich, Switzerland

M. Fujioka · K. Nishio · K. Okuchi
Emergency and Critical Care Medical Center, Nara Medical University, Nara, Japan

K. Irie · Y. Akitake · K. Mishima · C. Muroi · K. Iwasaki
Institute for Aging and Brain Sciences, Fukuoka University, Fukuoka, Japan

F. Banno · K. Kokame · T. Miyata
Research Institute, National Cerebral and Cardiovascular Center, Suita, Japan

B. K. Siesjö
Laboratory for Experimental Brain Research, Lund University, Lund, Sweden

Introduction

The post-ischemic inflammation incites stroke evolution [15, 16, 19–21, 32]. An ischemic insult triggers leukocytes infiltration and astrocyte and microglia activations in the affected brain, leading to the increase of the high-mobility group box1 (HMGB1) in the plasma and brain of the stroke model [19, 21]. The HMGB1 is a potent proinflammatory cytokine secreted by blood-immune [23, 29, 45] and brain-glial cells [35]. This extracellular HMGB1 further activates monocytes/macrophages [3, 34], neutrophils [1, 34], microvascular endothelial cells [12], astrocytes [36] and microglia [24], amplifies the systemic and brain inflammation, and extends the ischemic brain damage into the penumbra [19, 21, 24, 27, 33, 38].

Within the ischemic brain vasculature after middle cerebral artery occlusion (MCAO), circulating platelets [2, 28] and leukocytes [9, 28, 31] are activated, inducing microvascular obstructions and inflammation. In the initial activations of platelet and leukocyte on ischemic endothelium, a large multimeric adhesive glycoprotein von Willebrand factor (VWF) plays a central role. The VWF multimer tethers platelets on the vascular endothelial surface, leading to platelet activation [40]. This platelet-decorated VWF multimer string bound to endothelium supports leukocytes tethering, rolling and transmigration on stimulated vascular endothelial cells, and links thrombosis to inflammation [5, 7, 37]. The platelet binding affinity of VWF increases with increasing length of the VWF multimer strand and with high fluid shear stress [40, 44]. Accordingly, the longest multimer termed ultra-large VWF (ULVWF; secreted by vascular endothelium upon stimulation) exerts its maximum prothrombotic and pro-inflammatory functions in the microvasculture or stenotic vessels under high shear stress condition [30, 40, 41, 43].

A disintegrin and metalloproteinase with thrombospondin type-1 motifs 13 (ADAMTS13) inhibits these VWF functions by cleaving the Tyr1605–Met1606 bond in the A2 domain of the VWF [13, 41]. Physiologically, circulating ADAMTS13 cleaves the ULVWF secreted from endothelial cells, releasing tethered platelets and VWF fragments [11]. In a setting of on-going thrombus formation, the high shear stress induced at the stenotic vasculature stretches plasma-derived VWF multimers (smaller than ULVWF) on the thrombus surface. The extended VWF multimers involved in the platelet thrombosis are consequently cleaved by ADAMTS13 [41]. Notably, by decreasing the interaction between the ULVWF–platelet strands and leukocytes, ADAMTS13 reduces leukocytes adhesion and extravasation on the stimulated vascular wall and down-regulates tissue inflammation [5, 7, 37]. ADAMTS13 deficiency in humans increases the circulating ULVWF resulting in thrombotic thrombocytopenic purpura (TTP) [17, 41]. The TTP manifests fever and neurological deficits associated with VWF–platelet microthrombus formation in the brain. This implies that ADAMTS13 plays a role in inflammation after brain ischemia in TTP patients.

Early studies have shown that ADAMTS13 deficiency aggravates ischemic brain damage in experimental stroke models [14, 48]. We revealed that in the ADAMTS13-deficient mice after a brief focal ischemia the post-ischemic hypoperfusion was significantly amplified partly because of enhanced microvascular plugging by VWF–platelet–leukocyte complex [14]. However, it still remains unclear if an enhanced inflammatory reaction is involved in the deterioration of ischemic brain injury under ADAMTS13 deficiency. Here, we investigated whether ADAMTS13 gene deletion intensifies the increase of extracellular HMGB1, a hallmark of post-stroke inflammation, and exacerbates the brain damage after ischemia–reperfusion.

Materials and methods

Animals

The effect of ADAMTS13 gene deletion on inflammation after brain ischemia was investigated using male ADAMTS13KO and littermate WT mice in an SV129 genetic background, originally generated as a TTP model by our study group [4]. Studies using KO ($n = 31$) and WT ($n = 31$) mice (8–10 weeks of age, 20–23 g of body weight) were approved by the institutional ethics committee. The genotype of each animal was kept unspecified until all experiment's completion.

Middle cerebral artery occlusion

Thirty-minute MCAO by thread insertion from the common carotid artery was induced in KO ($n = 21$) and WT ($n = 21$) mice as previously described [14, 19–21]. Mice were anesthetized with 2% halothane for induction and maintained on 1% halothane in 70% N_2O and 30% O_2 by face mask. Body temperature was maintained at 36.5–37.0°C during surgery. Successful left MCAO was confirmed according to the following criteria: (1) rCBF in the left cerebral cortex at the thread insertion less than 20% of the pre-MCAO rCBF, and (2) consistent presence of significant ischemic neurological symptoms of the left cerebral hemisphere, characterized by right paresis and right circling behavior, during 30-min MCAO. The MCAO surgery was performed within 7 min without bleeding. The anesthesia was discontinued during 30-min MCAO. There were no statistically significant differences in body temperature between the two groups immediately before or after the thread insertion, or 10, 20, and 30 min after

MCAO. The thread was removed under re-anesthesia after 30-min MCAO. Sham surgery in KO ($n = 10$) and WT ($n = 10$) involved temporary insertion (1 s) of the thread into the left common carotid artery without MCAO. There were no statistical differences in prothrombin time or survival rate between KO and WT mice at 24 h after MCAO (Table 1).

Regional cerebral blood flow

The rCBF was measured by laser Doppler flowmetry (LDF) (ALF21, Advance Co., Tokyo, Japan) as previously described [14, 20]. The LDF probe was placed through a guide cannula into the left cerebral cortex stereotaxically (0.22 mm posterior and 2.5 mm lateral from bregma; 1.5 mm depth from the skull surface) on a stereotaxic instrument (Narishige Scientific Instrument Lab: SR-5 M, Tokyo) under anesthesia (pentobarbital 50 mg/kg, i.p.) 24 h before MCAO or sham surgery. The rCBF was monitored in all animals continuously from 30 min before MCAO until immediately after reperfusion. In randomly selected animals, the rCBF was repeatedly recorded over time within 24 h after MCAO. The rCBF during occlusion and reperfusion was expressed as percentages of the preMCAO LDF baseline value.

Infarct volume and neurological deficit

The brains were sectioned coronally (four 2-mm thick slices) according to a mouse brain matrix 24 h after MCAO (KO, $n = 14$ and WT, $n = 15$) or sham operation (KO, $n = 5$ and WT, $n = 5$). The infarct area was measured in each slice stained with 2,3,5 triphenyltetrazolium chloride with an image analysis system (NIH Image, version 1.63), and the infarct volume was calculated [14, 19–21]. Neurological deficit score ranging from 0 (normal motor function) to 5 (no spontaneous motor activity) was measured at 24 h after MCAO [14, 19, 21] (Table 1).

Plasma HMGB1 measurement

The plasma HMGB1 protein was evaluated by western blot 24 h after MCAO. Plasma samples were fractionated by sodium dodecyl sulfate (SDS)-polyacrylamide gel electrophoresis, and HMGB1 levels were determined by immunoblotting with respect to a standard curve, with recombinant HMGB1 as a reference (Sigma-Aldrich, Tokyo) [19, 21]. A blood sample (500 μL) was taken from each experimental animal via inferior vena cava 24 h after MCAO (KO, $n = 11$ and WT, $n = 12$) or sham surgery (KO, $n = 10$ and WT, $n = 10$). The sample was centrifuged (3,000 rpm at 4°C for 10 min), and the supernatant (200 μL) was further centrifuged (15,000 rpm at 4°C for 20 min). SDS sample buffer [125 mmol/L Tris (pH 6.8), 2% SDS, 20% glycerol, 0.0001% bromophenol blue, and 10% β-mercaptoethanol] (100 μL) was added to the plasma extract solution (100 μL), and the resultant sample was heated at 95°C for 5 min. Protein (15 μg) was separated by SDS–polyacrylamide gel electrophoresis (20% gel). Blotting was performed at 2 mA/cm^2 by semi-dry type blotting (Bio-Rad, Tokyo, Japan). The blots were blocked with 5% non-fat dry milk in Tris-buffered saline in 0.1% Tween 20 (TBS-T) at 4°C and incubated with goat polyclonal anti-HMGB1 primary antibody (1:200) (Santa Cruz Biotechnology, Santa Cruz, CA, USA) in TBS-T, followed by bovine anti-goat IgG (heavy chain and light chain [H + L]) alkaline phosphatase conjugate (1:1000) in TBS-T. The blots were visualized with the use of alkaline phosphatase color reagents. The signal intensity of the blots was measured with an image analysis system (NIH Image, version 1.63).

Double immunohistochemical staining for HMGB1/NeuN and HMGB1/MPO

Double immunofluorescent labeling for HMGB1 with NeuN or MPO on paraffin-embedded 5-μm coronal sections

Table 1 Effect of ADAMTS13 gene deletion on brain ischemia in mice after 30-min MCAO and 23.5-h reperfusion

	WT		KO
Brain infarct volume (mm^3)	12.0 ± 2.0 ($n = 15$)	$p < 0.05$[a]	28.5 ± 5.8 ($n = 14$)
Neurological deficit score	1.3 ± 0.2 ($n = 15$)	$p < 0.05$[a]	1.9 ± 0.2 ($n = 14$)
Prothrombin time (s)	12.1 ± 0.8 ($n = 7$)	ns	11.6 ± 0.9 ($n = 6$)
Survival rate (%)	95.2 ($n = 20/21$)	ns	90.4 ($n = 19/21$)

The values are expressed as the mean ± SEM. Neurological deficit score, score 0; normal motor function, 1; flexion of torso and of contralateral forelimb upon lifting of the animal by the tail, 2; circling to the ipsilateral side but normal posture at rest, 3; circling to the ipsilateral side, 4; rolling to the ipsilateral side, 5; leaning to the ipsilateral side at rest (no spontaneous motor activity)

ns Statistically not significant

[a] Student *t* test

of the mouse brain was analyzed by fluorescence microscopy (Nikon, AZ-FL, Tokyo, Japan). At 24 h after MCAO (KO, $n = 5$; WT, $n = 5$) or sham surgery (KO, $n = 5$; WT, $n = 5$), mice were humanely perfused transcardially with saline and 4% paraformaldehyde. The brains were removed of fat and water using an autodegreasing unit (RH-12; Sakura Seiko Co, Tokyo) and embedded in paraffin. Subsequently, 5-μm sections were mounted on slides and dried at 37°C for 1 day. After deparaffinization and rehydration, the sections were incubated with primary antibodies of biotinylated anti-mouse NeuN (1:200; Chemicon International, Temecula, CA, USA) or rabbit polyclonal anti-MPO (1:200; DAKO Inc., Carpinteria, CA, USA) and of goat polyclonal anti-HMGB1 (1:200; Santa Cruz Biotechnology, Santa Cruz, CA, USA) overnight at 4°C. Sections were then incubated with donkey anti-goat IgG-FITC secondary antibody (1:200; Santa Cruz Biotechnology) for 1 h, and thereafter with goat anti-rabbit IgG-Texas red secondary antibody (1:200; Santa Cruz Biotechnology) or Ultra avidine Texas Red (1:200; Leinco Technologies) for 1 h. The sections were imaged and analyzed. The histological findings were evaluated by neuropathologists until a consensus was obtained. The fluorescence intensity (for cells positive to NeuN, MPO, or HMGB1) in five randomly selected areas (150 μm × 200 μm for each) from the region of interest in the ischemic cerebral cortex (as indicated in Figs. 2, 3) was evaluated with an image analysis system (NIH Image, version 1.63) with the corresponding non-ischemic contralateral regions as a control, and the relative fluorescence intensity was calculated. In ischemic stroke, the necrotic core is surrounded by a zone of reactive/inflammatory cytosis which can extend the initial insult into the penumbra with delayed cell death. Based on this concept, the region of interest in the cortical penumbra for the fluorescence evaluation was decided as indicated.

Statistical analysis

Data are presented as mean ± standard error of mean (SEM). For multiple pairwise comparisons in parametric analysis, two-way analysis of variance (ANOVA) followed by Tukey–Kramer's test was performed. When only two groups were compared, Student's *t* test was used. Probability values of <0.05 were considered statistically significant.

Results

Brain infarction

The ADAMTS13 gene knockout (ADAMTS13KO) mice group had a significantly larger volume of brain infarction compared with the wild-type (WT) following 23.5-h reperfusion after 30-min MCAO (Student's *t* test) (Table 1). No ischemic brain damage was observed in either KO or WT mice after sham operation.

Neurological deficits

ADAMTS13KO mice had more severe neurological deficits than the WT (Student's *t* test) 24 h after MCAO (Table 1).

Regional cerebral blood flow

The rCBF showed no statistical differences between the two groups during MCAO or immediately after reperfusion. However, the rCBF in ADAMTS13KO mice progressively decreased significantly more markedly compared to WT during the first 30-min reperfusion (Tukey–Kramer's test). 24 h after MCAO, the rCBF in KO mice remained significantly lower compared to WT (Student's *t* test) (Table 2).

ADAMTS13 gene deletion enhances post-ischemic increase of plasma HMGB1

A 30-min MCAO and 23.5-h reperfusion significantly increased the plasma HMGB1 level both in ADAMTS13KO and WT mice as compared to sham operation (Fig. 1). However, this increase of plasma HMGB1 after MCAO was more markedly enhanced in ADAMTS13KO mice than in WT (Tukey–Kramer's test).

ADAMTS13 gene deletion intensifies post-ischemic brain inflammation and neuronal death

Double immunohistochemical staining for HMGB1/NeuN and HMGB1/MPO

The qualitative analysis of double immunofluorescent labeling for HMGB1 with NeuN (neuron-specific nuclear protein) or MPO (myeloperoxidase) on the cortical tissue 24 h after MCAO or sham operation showed that (1) the number of neurons immunoreactive to NeuN in the ischemic penumbra decreased more in ADAMTS13KO mice compared to WT (Fig. 2), (2) HMGB1 immunoreactivity disappeared in the ischemic neuronal nuclei in both KO and WT mice, suggestive of a translocation of HMGB1 from neuronal nucleus either to neuronal cytoplasm or to extracellular space (Fig. 2), and (3) cells with co-expression of MPO (a marker for neutrophils, macrophages and/or microglia) and HMGB1 appeared more prominently in the ischemic penumbra in ADAMTS13KO mice than in WT (Fig. 3).

Table 2 Effect of ADAMTS13 gene deletion on regional cerebral blood flow (rCBF) in mice of 30-min MCAO model

	WT ($n = 6$)		KO ($n = 7$)
Time (min)			
Baseline	100.0 ± 0	ns	100.0 ± 0
0	13.6 ± 4.6	ns	13.2 ± 2.0
10	17.9 ± 3.4	ns	22.4 ± 6.3
20	17.7 ± 5.2	ns	19.3 ± 5.7
30	16.8 ± 4.7	ns	18.6 ± 3.5
Reperfusion	114.3 ± 19.1	ns	88.1 ± 8.1
40	90.5 ± 12.7	$p < 0.05$[a]	48.4 ± 8.4
50	93.8 ± 11.3	$p < 0.01$[a]	35.4 ± 7.7
60	83.2 ± 6.8	$p < 0.01$[a]	28.1 ± 4.7
Time (hour)			
24	72.9 ± 13.9	$p < 0.05$[b]	37.2 ± 5.9

rCBF values are expressed as the mean ± SEM (% of baseline)

[a] Turkey-Kramer's test after two-way repeated measures ANOVA [$F(8,98) = 5.841$, $p < 0.0001$)]

[b] Student's t test

Relative fluorescent intensity of NeuN, MPO and HMGB1

The relative fluorescent intensity (%) in the ischemic cerebral cortex 24 h after MCAO was significantly decreased for NeuN in ADAMTS13KO mice compared to WT [57.5 ± 8.7 in KO vs. 93.2 ± 5.5 in WT ($p < 0.05$, student's t test)], and increased for both MPO and HMGB1 more in ADAMTS13KO mice than in WT [KO vs. WT: 557.7 ± 139.8 vs. 310.4 ± 131.7 for MPO, and 159.7 ± 46.5 vs. 70.2 ± 35.1 for HMGB1 (although not statistically significant)].

Discussion

The (UL)VWF, the substrate of ADAMTS13, recruits platelets and leukocytes onto the injured vascular endothelium, and mediates microvascular plugging and enhances the tissue inflammation [5, 7, 30, 37, 40, 41, 43, 44]. ADAMTS13 inhibits these prothrombotic and proinflammatory functions of (UL)VWF [7, 13, 41]. Our current study implies that ADAMTS13 gene deletion amplifies systemic and brain inflammatory responses against brain ischemia–reperfusion enhancing a potent cytokine HMGB1 neurotoxicity, leads to progressive decline of post-ischemic cerebral blood reflow, and exacerbates ischemic brain injury. ADAMTS13 may play a neuroprotective role against inflammation in ischemic stroke.

ADAMTS13 deficiency may promote inflammation by activating platelets, leukocytes, and vascular endothelium after brain ischemia–reperfusion. Responding to ischemia–

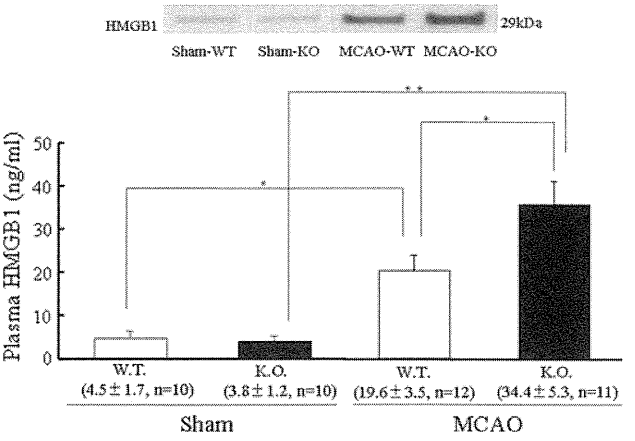

Fig. 1 Effect of ADAMTS13 gene deletion on plasma HMGB1 in mice after 30-min MCAO. The plasma HMGB1 protein was evaluated by western blot. Transient focal ischemia of 30-min MCAO followed by 23.5-h reperfusion significantly increased the plasma HMGB1 level both in ADAMTS13KO and WT mice when compared to sham operation [plasma HMGB1 (ng/ml): MCAO-KO; 34.4 ± 5.3 vs. sham-KO; 3.8 ± 1.2, $p < 0.01$, and MCAO-WT; 19.6 ± 3.5 vs. sham-WT; 4.5 ± 1.7, $p < 0.05$, Tukey–Kramer's test after two-way ANOVA (F (1,40) = 38.401, $p < 0.01$)]. This increase of plasma HMGB1 at 24 h after MCAO was more markedly enhanced in ADAMTS13KO mice than in WT [MCAO-KO; 34.4 ± 5.3 vs. MCAO-WT; 19.6 ± 3.5, $p < 0.05$, Tukey–Kramer's test after two-way ANOVA ($F(1,40) = 4.296$, $p < 0.05$)]. Sham-WT $n = 10$, Sham-KO $n = 10$, MCAO-WT $n = 12$, MCAO-KO $n = 11$. Values are expressed as the mean ± SEM. $*p < 0.05$, $**p < 0.01$, Tukey–Kramer's test after two-way ANOVA

reperfusion, the stimulated vascular endothelial cells secrete ULVWF [44]. Binding of VWF to the platelet membrane glycoprotein initiates a signaling cascade that causes platelet activation [25, 46]. The activated platelets release multiple proinflammatory factors, mitogenic mediators, metalloproteinases, and reactive oxygen species, and stimulate the leukocytes and endothelium to incite inflammatory reactions [8, 10]. Further, the platelet–(UL)VWF string directly supports the leukocyte transmigration into the inflammatory tissue [5, 7, 37]. Thus, the VWF-cleaving protease ADAMTS13 plays a role as an anti-inflammatory factor, and therefore its deficiency can exaggerate the post-ischemic inflammation.

In ADAMTS13KO mice after a cerebral ischemia, the plasma HMGB1 increased more and the HMGB1-expressing immune cells appeared more prominent in the cortical penumbra than in WT. The increased extracellular HMGB1 may contribute to secondary ischemic brain damage in ADAMTS13KO mice. The HMGB1, a DNA-binding protein, is a central proinflammatory cytokine [29]. Upon inflammatory signals, the chromosomal HMGB1 relocates into cytoplasmic secretory lysosomes and is secreted into the immunological synapse [29] or into the extracellular space by monocytes/macrophages [45], neutrophils [23], mature dendritic cells [29], natural killer cells

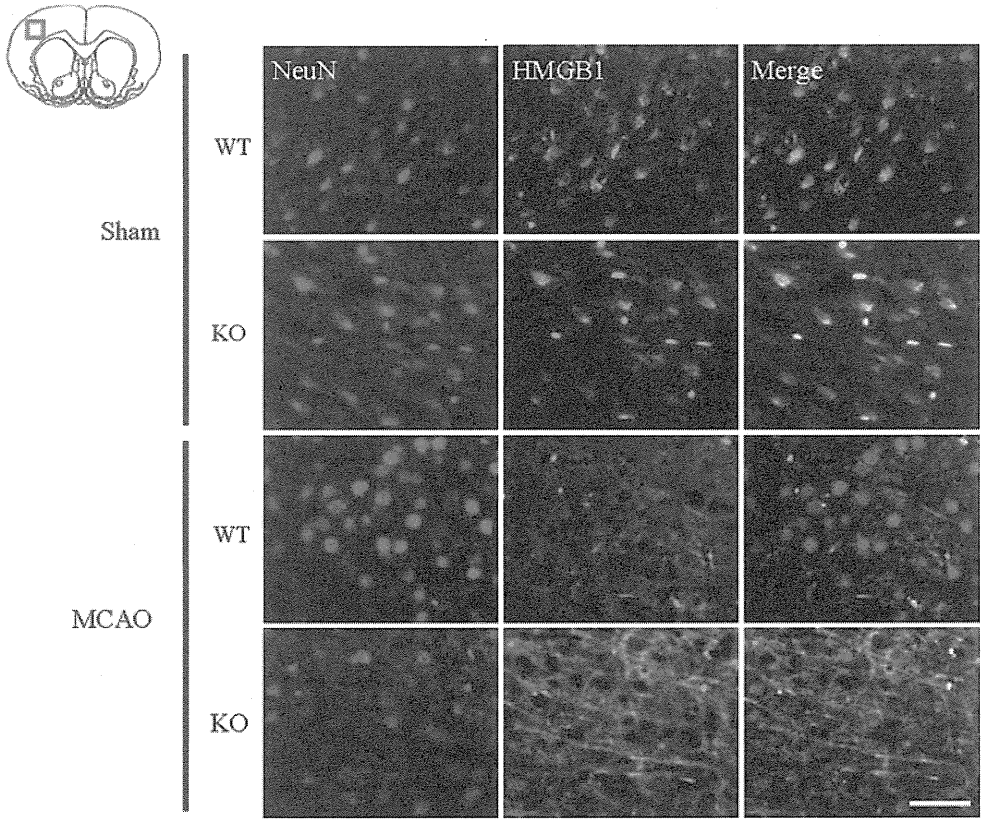

Fig. 2 Effect of ADAMTS13 gene deletion on NeuN positive cells expressing HMGB1 in mice brain after 30-min MCAO. Qualitative analysis of double immunofluorescent labeling for HMGB1 with NeuN on the brain tissue 24 h after MCAO showed that the number of neurons immunoreactive to NeuN in the ischemic cortical penumbra decreased more in ADAMTS13KO mice than WT. The HMGB1 immunoreactivity disappeared in the ischemic neuronal nuclei in both KO and WT mice, suggesting that neuronal-nuclear HMGB1 translocated into either the neuronal cytoplasm or the extracellular space. In addition, the HMGB1 immunoreactivity seemed to increase in the ischemic cortical tissue in the ADAMTS13KO mice, indicating a possibility that non-neuronal HMGB1 positive cells were activated in the KO mice compared to the WT ($n = 5$ in each group). *Scale bar* 50 μm. NeuN positive cells *red*, HMGB1 positive cells *green*, merge *yellow*

[29], and glia [35]. HMGB1 also leaks from necrotic cells [42] and ischemic neurons [38]. The extracellular HMGB1 binds to its receptors, RAGE (receptor for advanced glycation end products) [22], Toll-like receptor 2 (TLR2), and TLR4 [34], recapitulates the intracellular signaling cascades initiated by early proinflammatory stresses, and thus propagates continuous proinflammatory responses [3, 22, 29, 34, 42]. Naturally, high blood HMGB1 correlates with the severity of systemic inflammation [29, 45].

After brain ischemia, extracellular HMGB1 increases rapidly in the blood and central nervous system, and induces neuroinflammation [24, 38]. HMGB-1 early released from the striatal ischemic core can bind to RAGE that is robustly expressed in the peri-infarct region, and extend the ischemic brain injury [38]. HMGB1-RAGE signaling in infiltrating macrophages and activated microglia seemingly mediate neuronal death evolution in the ischemic penumbra [33]. The HMGB1 inhibition in the brain or systemic circulation protects the blood–brain barrier and the brain from ischemia [24, 27, 33, 47]. Inhibition of leukocytes and microglia results in decreased HMGB1 levels in the brain and plasma, reduces apoptosis in the ischemic brain, and improves brain atrophy and neurologic deficits [19, 21]. Therefore, the increased extracellular HMGB1 in the blood and brain of ADAMTS13KO mice as observed in our study can exacerbate ischemic brain injury by intensifying systemic and brain inflammation. Interestingly, the platelet intracellular HMGB1 is exported to the external surface of the plasma membrane upon its activation [39]. Accordingly, the activated platelet may be an additional source of the exceedingly increased plasma HMGB1 in ADAMTS13KO mice after brain ischemia, where enhanced VWF–platelet interactions develop [14]. We suggest that ADAMTS13 deficiency multiplies secondary insults after brain ischemia by up-regulating (UL)VWF-mediating inflammation and enhancing HMGB1 neurotoxicity in the systemic and local environments.

This study suggests a potential therapy with ADAMTS13 for acute ischemic stroke by breaking a vicious circle

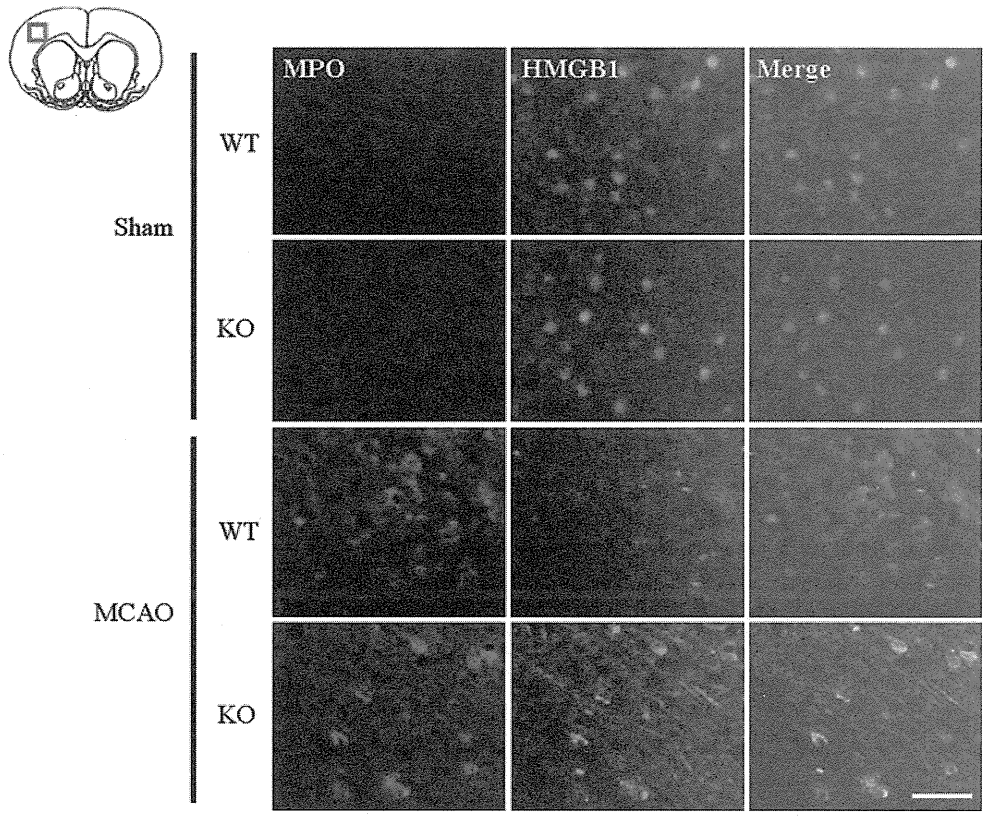

Fig. 3 Effect of ADAMTS13 gene deletion on MPO positive cells expressing HMGB1 in mice brain after 30-min MCAO. Qualitative analysis of double immunofluorescent labeling for HMGB1 with MPO on the brain tissue 24 h after MCAO showed that cells co-expressing MPO and HMGB1 were more prominent in the ischemic cortical penumbra in KO mice than in WT ($n = 5$ in each group). *Scale bar* 50 μm. MPO positive cells *red*, HMGB1 positive cells *green*, merge *yellow*

of thrombosis and inflammation. The (UL)VWF–platelet string interacts with leukocytes, and provokes inflammation [5, 7, 37]. The inflammation induces the endothelial-ULVWF secretion [44]. The proinflammatory cytokines from leukocytes and endothelial cells [such as tumor necrosis factor (TNF)-α and interleukin (IL)-8] stimulate the endothelial ULVWF release and IL-6 protects the ULVWF from cleavage [6]. This would increase the number of ULVWF multimers in plasma sufficiently to aggregate platelets and on vascular endothelial surface to tether platelets and leukocytes onto the endothelium, providing a linkage between thrombosis and inflammation. Of note, HMGB1 stimulates the monocytes/macrophages [3, 34], neutrophils [1, 34] and glial cells [24, 36, 38] to produce TNF-α, IL-1, IL-6 and/or IL-8, and incites the microvascular endothelial cells [12, 38] to express TNF-α, IL-8 and various adhesion molecules. Namely, the increased plasma HMGB1 in ADAMTS13-deficient mice can upregulate ULVWF, and thus reinforce the association between inflammation and thrombosis. ADAMTS13 may prevent stroke evolution by interfering with the crosstalk between thrombosis and inflammation.

Thrombolytic therapy using tissue plasminogen activator (tPA) for acute stroke has limitations in the therapeutic time window and in the drug dosage due to the risk of hemorrhagic transformation [18]. Further, tPA directly exerts neurotoxicity in the ischemic brain [26]. We suggest that a regulation of the interaction between (UL)VWF–platelet and leukocyte using ADAMTS13 may become a novel therapeutic option in acute brain ischemia. ADAMTS13 does not dissolve the VWF–platelet–primary hemostatic thrombus in the absence of pathologically high fluid shear stress. Therefore, ADAMTS13 may be particularly well suited for acute ischemic stroke without increasing hemorrhagic complications. An early experimental study [48] together with our preliminary data (not shown) demonstrated that recombinant human ADAMTS13 administration reduced infarct volume in stroke model in a VWF-dependent manner without producing cerebral hemorrhage.

This study has several limitations. For example, the reduction of cerebral blood reflow in ADAMTS13KO mice after ischemic insult was continuous and higher than that observed in WT. Therefore, even without the amplified inflammation with HMGB1 neurotoxic effects, only the difference in the blood flow recovery might explain the following more deleterious events in the ischemic brain of ADAMTS13-deficient mice compared to WT. The enhanced elevation of the plasma HMGB1 under ADAMTS13 deficiency after brain ischemia might be also explained simply by the more exacerbated brain damage, regardless of the theoretically intensified interactions between the platelet–(UL)VWF strands and the leukocytes without VWF cleaving protease. The future study required to clarify these issues would include chronological data

evaluations in the stroke experiments with permanent ischemic procedure (deleting the reperfusion effect) or with enhancing/inhibiting HMGB1 activities by drugs or genetic manipulations.

Conclusions

A gene deletion of ADAMTS13 renders mice more vulnerable to brain ischemia–reperfusion injury than their wild-type counterparts, when subjected to 30-min MCAO. This preliminary study suggests that ADAMTS13 deficiency may exacerbate systemic and neuronal inflammation after brain ischemia via VWF-dependent pathway, although this remains still hypothetical. Further studies are warranted to better characterize the role of ADAMTS13 in brain ischemia–reperfusion and to provide a novel therapeutic approach for ischemic stroke by regulating VWF-dependent inflammation as well as microvascular plugging.

References

1. Abraham E, Arcaroli J, Carmody A, Wang H, Tracey KJ (2000) HMG-1 as a mediator of acute lung inflammation. J Immunol 165:2950–2954
2. Abumiya T, Fitridge R, Mazur C, Copeland BR, Koziol JA, Tschopp JF, Pierschbacher MD, del Zoppo GJ (2000) Integrin alpha(IIb)beta(3) inhibitor preserves microvascular patency in experimental acute focal cerebral ischemia. Stroke 31:1402–1409
3. Andersson U, Wang H, Palmblad K, Aveberger AC, Bloom O, Erlandsson-Harris H, Janson A, Kokkola R, Zhang M, Yang H, Tracey KJ (2000) High mobility group 1 protein (HMG-1) stimulates proinflammatory cytokine synthesis in human monocytes. J Exp Med 192:565–570
4. Banno F, Kokame K, Okuda T, Honda S, Miyata S, Kato H, Tomiyama Y, Miyata T (2006) Complete deficiency in ADAMTS13 is prothrombotic, but it alone is not sufficient to cause thrombotic thrombocytopenic purpura. Blood 107:3161–3166
5. Bernardo A, Ball C, Nolasco L, Choi H, Moake JL, Dong JF (2005) Platelets adhered to endothelial cell-bound ultra-large von Willebrand factor strings support leukocyte tethering and rolling under high shear stress. J Thromb Haemost 3:562–570
6. Bernardo A, Ball C, Nolasco L, Moake JF, Dong JF (2004) Effects of inflammatory cytokines on the release and cleavage of the endothelial cell-derived ultralarge von Willebrand factor multimers under flow. Blood 104:100–106
7. Chauhan AK, Kisucka J, Brill A, Walsh MT, Scheiflinger F, Wagner DD (2008) ADAMTS13: a new link between thrombosis and inflammation. J Exp Med 205:2065–2074
8. Davi G, Patrono C (2007) Platelet activation and atherothrombosis. N Engl J Med 357:2482–2494
9. Del Zoppo GJ, Schmid-Schonbein GW, Mori E, Copeland BR, Chang CM (1991) Polymorphonuclear leukocytes occlude capillaries following middle cerebral artery occlusion and reperfusion in baboons. Stroke 22:1276–1283
10. Dole VS, Bergmeier W, Mitchell HA, Eichenberger SC, Wagner DD (2005) Activated platelets induce Weibel-Palade-body secretion and leukocyte rolling in vivo: role of P-selectin. Blood 106: 2334–2339
11. Dong JF, Moake JL, Nolasco L, Bernardo A, Arceneaux W, Shrimpton CN, Schade AJ, McIntire LV, Fujikawa K, López JA (2002) ADAMTS-13 rapidly cleaves newly secreted ultralarge von Willebrand factor multimers on the endothelial surface under flowing conditions. Blood 100:4033–4039
12. Fiuza C, Bustin M, Talwar S, Tropea M, Gerstenberger E, Shelhamer JH, Suffredini AF (2003) Inflammation-promoting activity of HMGB1 on human microvascular endothelial cells. Blood 101:2652–2660
13. Fujikawa K, Suzuki H, McMullen B, Chung DP (2001) Purification of human von Willebrand factor-cleaving protease and its identification as a new member of the metalloproteinase family. Blood 98:1662–1666
14. Fujioka M, Hayakawa K, Mishima K, Kunizawa A, Irie K, Higuchi S, Nakano T, Muroi C, Fukushima H, Sugimoto M, Banno F, Kokame K, Miyata T, Fujiwara M, Okuchi K, Nishio K (2010) ADAMTS13 gene deletion aggravates ischemic brain damage: a possible neuroprotective role of ADAMTS13 by ameliorating postischemic hypoperfusion. Blood 115:1650–1653
15. Fujioka M, Taoka T, Matsuo Y, Hiramatsu KI, Sakaki T (1999) Novel brain ischemic change on MRI. Delayed ischemic hyperintensity on T1-weighted images and selective neuronal death in the caudoputamen of rats after brief focal ischemia. Stroke 30:1043–1046
16. Fujioka M, Taoka T, Matsuo Y, Mishima K, Ogoshi K, Kondo Y, Tsuda M, Fujiwara M, Asano T, Sakaki T, Miyasaki A, Park D, Siesjö BK (2003) Magnetic resonance imaging shows delayed ischemic striatal neurodegeneration. Ann Neurol 54:732–747
17. Furlan M, Robles R, Galbusera M, Remuzzi G, Kyrle PA, Brenner B, Krause M, Scharrer I, Aumann V, Mittler U, Solenthaler M, Lammle B (1998) von Willebrand factor-cleaving protease in thrombotic thrombocytopenic purpura and the hemolytic-uremic syndrome. N Engl J Med 339:1578–1584
18. Hacke W, Kaste M, Bluhmki E, Brozman M, Davalos A, Guidetti D, Larrue V, Lees KR, Medeghri Z, Machnig T, Schneider D, von Kummer R, Wahlgren N, Toni D (2008) Thrombolysis with alteplase 3 to 4.5 hours after acute ischemic stroke. N Engl J Med 359: 1317–1329
19. Hayakawa K, Mishima K, Irie K, Hazekawa M, Mishima S, Fujioka M, Orito K, Egashira N, Katsurabayashi S, Takasaki K, Iwasaki K, Fujiwara M (2008) Cannabidiol prevents a post-ischemic injury progressively induced by cerebral ischemia via a high-mobility group box1-inhibiting mechanism. Neuropharmacology 55:1280–1286
20. Hayakawa K, Mishima K, Nozako M, Hazekawa M, Irie K, Fujioka M, Orito K, Abe K, Hasebe N, Egashira N, Iwasaki K, Fujiwara M (2007) Delayed treatment with cannabidiol has a cerebroprotective action via a cannabinoid receptor-independent myeloperoxidase-inhibiting mechanism. J Neurochem 102:1488–1496
21. Hayakawa K, Mishima K, Nozako M, Hazekawa M, Mishima S, Fujioka M, Orito K, Egashira N, Iwasaki K, Fujiwara M (2008) Delayed treatment with minocycline ameliorates neurologic impairment through activated microglia expressing a high-mobility group box1-inhibiting mechanism. Stroke 39:951–958
22. Hori O, Brett J, Slattery T, Cao R, Zhang J, Chen JX, Nagashima M, Lundh ER, Vijay S, Nitecki D et al (1995) The receptor for advanced glycation end products (RAGE) is a cellular binding site for amphoterin. Mediation of neurite outgrowth and co-expression of rage and amphoterin in the developing nervous system. J Biol Chem 270:25752–25761
23. Ito I, Fukazawa J, Yoshida M (2007) Post-translational methylation of high mobility group box 1 (HMGB1) causes its cytoplasmic localization in neutrophils. J Biol Chem 282: 16336–16344

24. Kim JB, Sig Choi J, Yu YM, Nam K, Piao CS, Kim SW, Lee MH, Han PL, Park JS, Lee JK (2006) HMGB1, a novel cytokine-like mediator linking acute neuronal death and delayed neuroinflammation in the postischemic brain. J Neurosci 26:6413–6421
25. Kroll MH, Harris TS, Moake JL, Handin RI, Schafer AI (1991) von Willebrand factor binding to platelet GpIb initiates signals for platelet activation. J Clin Invest 88:1568–1573
26. Liu D, Cheng T, Guo H, Fernandez JA, Griffin JH, Song X, Zlokovic BV (2004) Tissue plasminogen activator neurovascular toxicity is controlled by activated protein C. Nat Med 10: 1379–1383
27. Liu K, Mori S, Takahashi HK, Tomono Y, Wake H, Kanke T, Sato Y, Hiraga N, Adachi N, Yoshino T, Nishibori M (2007) Anti-high mobility group box 1 monoclonal antibody ameliorates brain infarction induced by transient ischemia in rats. FASEB J 21:3904–3916
28. Lo EH, Dalkara T, Moskowitz MA (2003) Mechanisms, challenges and opportunities in stroke. Nat Rev Neurosci 4:399–415
29. Lotze MT, Tracey KJ (2005) High-mobility group box 1 protein (HMGB1): nuclear weapon in the immune arsenal. Nat Rev Immunol 5:331–342
30. Moake JL, Rudy CK, Troll JH, Weinstein MJ, Colannino NM, Azocar J, Seder RH, Hong SL, Deykin D (1982) Unusually large plasma factor VIII: von Willebrand factor multimers in chronic relapsing thrombotic thrombocytopenic purpura. N Engl J Med 307:1432–1435
31. Mori E, del Zoppo GJ, Chambers JD, Copeland BR, Arfors KE (1992) Inhibition of polymorphonuclear leukocyte adherence suppresses no-reflow after focal cerebral ischemia in baboons. Stroke 23:712–718
32. Mori T, Town T, Tan J, Tateishi N, Asano T (2005) Modulation of astrocytic activation by arundic acid (ONO-2506) mitigates detrimental effects of the apolipoprotein E4 isoform after permanent focal ischemia in apolipoprotein E knock-in mice. J Cereb Blood Flow Metab 25:748–762
33. Muhammad S, Barakat W, Stoyanov S, Murikinati S, Yang H, Tracey KJ, Bendszus M, Rossetti G, Nawroth PP, Bierhaus A, Schwaninger M (2008) The HMGB1 receptor RAGE mediates ischemic brain damage. J Neurosci 28:12023–12031
34. Park JS, Svetkauskaite D, He Q, Kim JY, Strassheim D, Ishizaka A, Abraham E (2004) Involvement of toll-like receptors 2 and 4 in cellular activation by high mobility group box 1 protein. J Biol Chem 279:7370–7377
35. Passalacqua M, Patrone M, Picotti GB, Del Rio M, Sparatore B, Melloni E, Pontremoli S (1998) Stimulated astrocytes release high-mobility group 1 protein, an inducer of LAN-5 neuroblastoma cell differentiation. Neuroscience 82:1021–1028
36. Pedrazzi M, Patrone M, Passalacqua M, Ranzato E, Colamassaro D, Sparatore B, Pontremoli S, Melloni E (2007) Selective proinflammatory activation of astrocytes by high-mobility group box 1 protein signaling. J Immunol 179:8525–8532
37. Pendu R, Terraube V, Christophe OD, Gahmberg CG, de Groot PG, Lenting PJ, Denis CV (2006) P-selectin glycoprotein ligand 1 and beta2-integrins cooperate in the adhesion of leukocytes to von Willebrand factor. Blood 108:3746–3752
38. Qiu J, Nishimura M, Wang Y, Sims JR, Qiu S, Savitz SI, Salomone S, Moskowitz MA (2008) Early release of HMGB-1 from neurons after the onset of brain ischemia. J Cereb Blood Flow Metab 28:927–938
39. Rouhiainen A, Imai S, Rauvala H, Parkkinen J (2000) Occurrence of amphoterin (HMG1) as an endogenous protein of human platelets that is exported to the cell surface upon platelet activation. Thromb Haemost 84:1087–1094
40. Ruggeri ZM (2007) The role of von Willebrand factor in thrombus formation. Thromb Res 120(Suppl 1):S5–S9
41. Sadler JE (2008) Von Willebrand factor, ADAMTS13, and thrombotic thrombocytopenic purpura. Blood 112:11–18
42. Scaffidi P, Misteli T, Bianchi ME (2002) Release of chromatin protein HMGB1 by necrotic cells triggers inflammation. Nature 418:191–195
43. Siedlecki CA, Lestini BJ, Kottke-Marchant KK, Eppell SJ, Wilson DL, Marchant RE (1996) Shear-dependent changes in the three-dimensional structure of human von Willebrand factor. Blood 88:2939–2950
44. Vischer UM (2006) von Willebrand factor, endothelial dysfunction, and cardiovascular disease. J Thromb Haemost 4:1186–1193
45. Wang H, Bloom O, Zhang M, Vishnubhakat JM, Ombrellino M, Che J, Frazier A, Yang H, Ivanova S, Borovikova L, Manogue KR, Faist E, Abraham E, Andersson J, Andersson U, Molina PE, Abumrad NN, Sama A, Tracey KJ (1999) HMG-1 as a late mediator of endotoxin lethality in mice. Science 285:248–251
46. Yin H, Liu J, Li Z, Berndt MC, Lowell CA, Du X (2008) Src family tyrosine kinase Lyn mediates VWF/GPIb-IX-induced platelet activation via the cGMP signaling pathway. Blood 112: 1139–1146
47. Zhang J, Takahashi HK, Liu K, Wake H, Liu R, Maruo T, Date I, Yoshino T, Ohtsuka A, Mori S, Nishibori M (2011) Anti-high mobility group box-1 monoclonal antibody protects the blood–brain barrier from ischemia-induced disruption in rats. Stroke 42:1420–1428
48. Zhao BQ, Chauhan AK, Canault M, Patten IS, Yang JJ, Dockal M, Scheiflinger F, Wagner DD (2009) von Willebrand factor-cleaving protease ADAMTS13 reduces ischemic brain injury in experimental stroke. Blood 114:3329–3334

ADAMTS13 safeguards the myocardium in a mouse model of acute myocardial infarction

Masaaki Doi[1,2]; Hideto Matsui[1]; Yukiji Takeda[3]; Yoshihiko Saito[3]; Maiko Takeda[4]; Yasunori Matsunari[1,5]; Kenji Nishio[6]; Midori Shima[2]; Fumiaki Banno[7]; Masashi Akiyama[7]; Koichi Kokame[7]; Toshiyuki Miyata[7]; Mitsuhiko Sugimoto[1]

[1]Department of Regulatory Medicine for Thrombosis, Nara Medical University, Kashihara, Japan; [2]Department of Pediatrics, Nara Medical University, Kashihara, Japan; [3]Department of Internal Medicine, Nara Medical University, Kashihara, Japan; [4]Department of Pathology, Nara Medical University, Kashihara, Japan; [5]Department of Anesthesiology, Nara Medical University, Kashihara, Japan; [6]Department of General Medicine, Nara Medical University, Kashihara, Japan; [7]Department of Molecular Pathogenesis, National Cerebral and Cardiovascular Center, Osaka, Japan

Dear Sirs,

The adhesive protein von Willebrand factor (VWF) plays an essential role on haemostasis (1–3). However, excessive functions of VWF could trigger thrombotic complications. To prevent this, the VWF-cleaving protease ADAMTS13 negatively regulates VWF function by reducing the size of VWF multimers, thereby decreasing their thrombogenic potential (1–3). Since the VWF function is dependent on shear stress (1–4), the relevance of ADAMTS13 may be more pronounced in the microcirculation (5), which is characterised by high shear stress created by blood flow. Indeed, functional deficiencies of ADAMTS13 cause thrombotic occlusion of the microvasculature, e.g. arterial capillaries, resulting in thrombotic thrombocytopenic purpura (3, 6).

Previously, we (7) and others (8, 9) reported that ADAMTS13 deficiency aggravates the extent of brain ischaemic stroke in a mouse model of ischaemia/reperfusion injury by middle cerebral arterial occlusion, suggesting that ADAMTS13 is neuroprotective. These studies demonstrated that ADAMTS13 plays a beneficial role in the microcirculation, which is critical for the preservation of organ functions, raising the possibility that ADAMTS13 might also play a role in coronary ischaemic events such as myocardial infarction. We investigated this possibility in an experimental model of acute myocardial infarction in ADAMTS13 gene deleted (*Adamts13 -/-*) mice.

Adamts13-/- (KO) mice were generated on C57BL/6 background by our study group, as described (7, 10). All mice were 12–14 weeks of age, healthy, fertile, and had body weights of 25–30 grams. Mouse experiments were done according to protocols approved by the Ethics Review Committee for Animal Experimentation of Nara Medical University. Researchers were blinded to the genotype of each animal until all studies were completed. Experimental acute myocardial infarction (AMI) in mice was induced as previously described (11). Briefly, following anesthesia by diethyl ether inhalation and insertion of a polyethylene tube into trachea, the left anterior descending coronary artery was ligated with a polyamide suture 2 mm from the tip of the left auricle, under thoracotomy with ventilator-assisted respiration. The same procedure without coronary artery ligation was performed in sham operations. In some experiments, recombinant human ADAMTS13 (3 μg/mouse, equivalent to 2,800 U/kg) was injected intravenously in 30 minutes (min) after the operation. This recombinant protein (designated as MDTCS) used was previously described (12). In brief, MDTCS spans from the metalloproteinase (M) domain to spacer (S) domain (amino acid residues 75–685); it possesses VWF-cleaving activity equivalent to whole ADAMTS13 molecule, as evaluated by the *in vitro* FRETS-VWF73 assay (12, 13)

Seven days after the coronary artery ligation, mouse cardiac (left-ventricular) function was evaluated by M-mode echocardiography. Subsequently, mice were sacrificed and their hearts were excised for histological analysis of myocardial infarction, as previously described (11). In brief, the ventricles of excised hearts were cut into 1-mm transverse slices and subjected to 2,3,5-triphenyltetrasolium chloride (TTC) and Azan staining. After inspection of the TTC specimens confirmed that myocardial infarction was successfully induced in mice, the "infarction ratio" was calculated from the Azan specimens by computer-assisted image analysis (analySIS software-version 2007; Olympus Soft Imaging Solutions). Infarction ratio was defined as the ratio of the area with fibrin deposition, corresponding to the infarct, to the total area of left ventricle.

Echocardiography revealed significantly increased end-diastolic diameter of left ventricle and reduced ejection fraction in knock-out (KO) mice, compared to wild-type mice, indicating that cardiac functions are relatively poor in KO mice (▶Fig. 1A). In addition, histological studies revealed significantly larger infarctions in myocardia of KO mice (▶Fig. 1B). Intravenous administration of recombinant human ADAMTS13 rescued the myocardial symptoms in KO mice (▶Fig. 1). Thus, our results clearly indicate that as in brain ischaemic stroke, ADAMTS13 plays a role in safeguarding the myocardium from coronary artery ischaemia.

During the preparation of this manuscript, a similar study by De Meyer et al. (14) appeared, demonstrating a protective effect of ADAMTS13 in mouse myocardial infarction. Those authors used a protocol for AMI induction somewhat different from ours: their study (14) and all previous brain stroke studies (7–9) employed a transient ischaemia/reperfusion model to experimentally induce ischaemia. By contrast, our approach to AMI induction, a persistent coronary artery ligation, represents a greater challenge regarding recovery of organ function following ischaemic damage, further highlighting the favorable effects of ADAMTS13. The successful res-

Correspondence to:
Mitsuhiko Sugimoto, MD or Hideto Matsui, MD
Department of Regulatory Medicine for Thrombosis
Nara Medical University
840 Shijo-cho, Kashihara, Nara 634–8521, Japan
Tel.: +81 744 23 9961, Fax: +81 744 23 9962
E-mail: sugi-ped@naramed-u.ac.jp;
hide-ped@naramed-u.ac.jp

Received: September 20, 2012
Accepted after minor revision: September 21, 2012
Prepublished online: October 10, 2012
doi:10.1160/TH12-09-0674
Thromb Haemost 2012; 108: 1236–1238

cue by recombinant ADAMTS13 in our more stringent system, in which it was administered just after the AMI induction, may imply the therapeutic potential for patients with acute coronary syndrome. Interestingly, our truncated recombinant molecule (MDTCS) was found to be fully effective *in vivo*, although the functional relevance of carboxyl-terminal domains of ADAMTS13, lacking in MDTCS, was controversial under flow conditions (15, 16).

The mechanisms underlying the beneficial effects of ADAMTS13 on myocardium remain poorly understood. As discussed in the previous brain stroke study (7), ADAMTS13 possibly prevents the thrombotic occlusion of microvasculature at the post-ischaemic reperfusion stage. In light of close associations between AMI and inflammation, the regulation of inflammatory mechanisms (17) could be critically involved in this regard. Indeed, De Meyer et al. (14) demonstrated that the recombinant ADAMTS13 infusion effectively reduced the neutrophil accumulation within infarct area, underscoring anti-inflammatory effects of ADAMTS13.

Since the activity of VWF (1–4) as well as ADAMTS13 (5) accelerates in a shear stress-dependent manner, the down-regulation of VWF-dependent inflammatory responses by ADAMTS13, such as leukocyte recruitment (17), is assumed to be more crucial in the microcirculation system, where blood flow creates a typical high shear stress. The small vessels of the microvasculature, such as arterial capillaries, can be plugged even by a single leukocyte. Such blockage could cause ischemic damage in vital organs even in the absence of thrombotic vessel occlusion by platelet aggregate formation. In fact, our histological examination did not reveal any increase in the incidence of thrombotic lesions in the microvessels in heart tissues of KO (results not shown).

Our results demonstrate that proper functional regulation of von Willebrand factor-dependent thrombotic or inflammatory responses by ADAMTS13 could contribute to better local microcirculation, which is crucial for healthy organ function. These findings suggest that ADAMTS13 may have therapeutic potential against acute coronary syndromes.

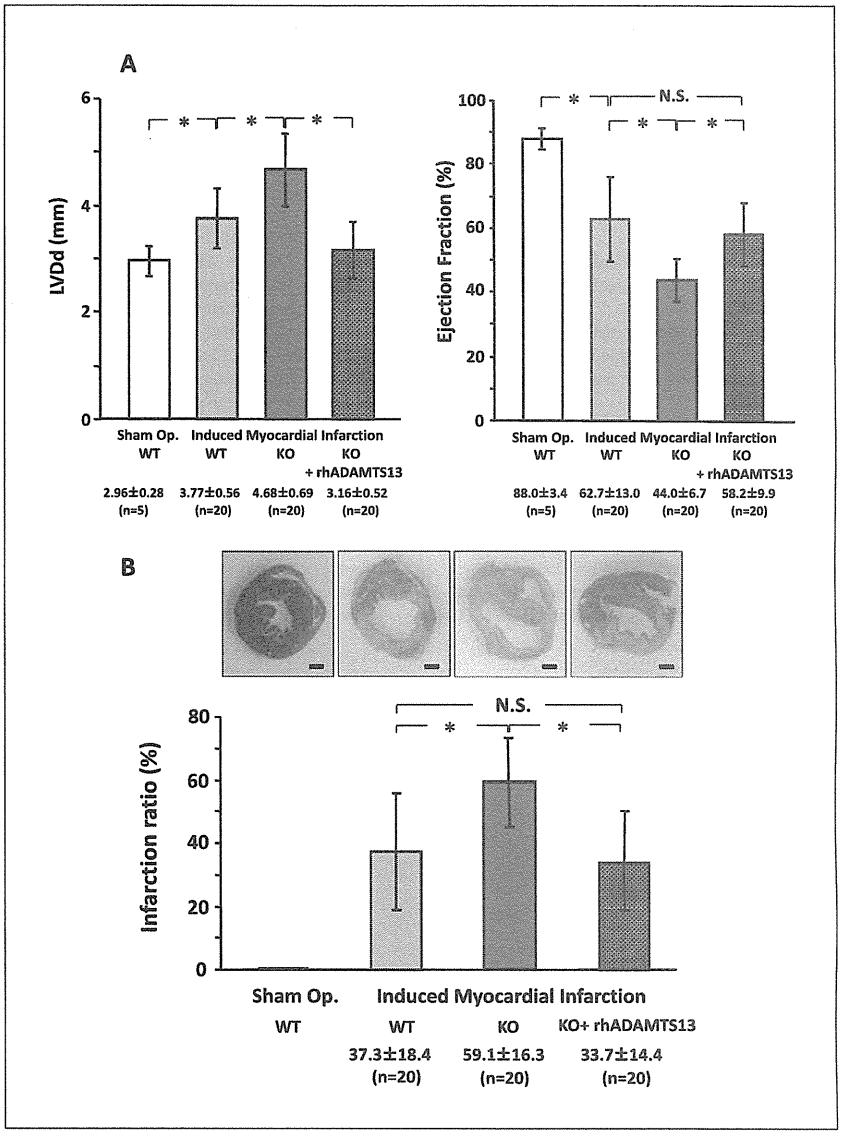

Figure 1: Evaluation of cardiac functions by echocardiography and histological evaluation in wild-type (WT) or ADAMTS13 KO mice with induced myocardial infarction. Acute myocardial infarction (AMI) was successfully induced in 20 WT mice (9 male, 11 female) and 20 KO mice (10 male, 10 female). In another 20 KO mice (8 male, 12 female), recombinant human ADAMTS13 (3 μg/mouse) was injected intravenously in 30 min after induction of AMI (KO+rhADAMTS13). Results of sham operation in five WT mice (2 male, 3 female) are also included in the figure. A) Statistical analysis of M-mode echocardiography indicates that KO mice exhibited significantly (*$p < 0.01$) increased left ventricular end-diastolic diameter (LVDd; left panel) and decreased ejection fraction (right panel) compared to WT. Note that the reduced cardiac functions observed in KO mice were improved by rhADAMTS13 injection, to become comparable (N.S.; not significant) with those of WT mice. All data are expressed as mean ± standard deviation. Differences between two groups of data were evaluated by Student's t-test. P-values < 0.05 were considered to denote statistical significance. B) Upper panels: representative microscopic images of transverse sections of ventricle subjected to Azan staining (original magnification; 20X, scale bars, 1 mm). Vital heart tissue is indicted in red; fibrin deposition, corresponding to the infarct area, is indicated in blue. In agreement with results of echocardiography, the infarction ratios (lower panel), corresponding to the upper images, indicated that myocardial infarctions were significantly (*$p < 0.01$) larger in KO mice than in WT mice, but were reduced by rhADAMTS13 injection, to become comparable (N.S.) with those of WT mice.